High-concentration point-defect chemistry: Statistical-thermodynamic approach applied to nonstoichiometric cerium dioxides

S. Ling
Corporate Research Science Laboratories, Exxon Research & Engineering Company, Annandale, New Jersey 08801
(Received 20 May 1993)

Many properties of crystalline solids are controlled by the presence of point defects. Traditionally the concentrations of these defects are calculated using mass action laws that describe the reactions among the defects and with the environment. This formulation, however, is not applicable in the high-defect-concentration regime because it is based on assumptions that are valid only at the limit of dilute defect concentration. In the present work a statistical thermodynamic approach is used to develop a defect chemistry formulation that has general applicability at all levels of defect concentrations. This is accomplished by deriving an expression for the virtual chemical potential of point defects from the Gibbs free energy that includes contributions from short-range and long-range Coulombic interactions, and from a configurational entropy that incorporates generalized exclusion effects. By balancing the chemical potentials of different species and the environment as required under thermodynamic equilibrium conditions, one can derive equations that govern the concentrations of defects. At the limit of low defect concentration, the current approach is shown to be equivalent to that of the traditional theory. This formulation is demonstrated by working out an example in detail using undoped $CeO_{2-\delta}$ as a model system. The concentrations of different species are calculated as functions of T and P_{O_2} using a numerical routine based on the conjugate gradient algorithm. The oxygen deficiency δ is obtained as the net concentrations of all oxygen vacancy containing species, and is found to be in good agreement with literature data. The effects of defect interactions and exclusions are discussed, and the thermodynamic activities of different species are calculated as functions of environmental parameters.

I. INTRODUCTION

Many properties of technologically important crystalline solids are controlled by the presence of point defects. These properties include color, diffusion, electronic and ionic conductance, luminescence, and magnetic susceptibility. As such, the study of the relationships between material properties and point defects is an area of active research.[1–3] Of central importance in these investigations is a quantitative knowledge of point-defect concentrations as functions of material compositions and environmental parameters. To date this understanding is provided by a defect chemistry formulation that has been described in detail by Kröger and Vink.[4,5] In this approach the defect concentrations are governed by a set of simultaneous equations, which include those that are derived from mass action laws describing the quasichemical defect reactions, and those that define additional physical constraints such as electrical neutrality, mass, and structural conservations.

The traditional defect chemistry formulation makes use of the assumption that the neighboring point defects are far apart.[4–7] Under this idealized condition the derivations are simplified by arguing that the interactions among the defects are negligible, and the spatial locations of the defects are random and statistically uncorrelated. It was then recognized that charged defects, such as those found in ionic crystals, can interact via long-range Coulombic forces. This small but non-negligible effect is accounted for by the Debye-Hückel correction,[8] in which the charge of a defect is found to be screened by that of other defects close by.[9–12] In any case, because of this basic assumption of large defect separation, the traditional approach is applicable only in the low concentration regime up to a level of $\sim 10^{-2}$ *mol fraction* defect content.[13,14] In actual practice, however, it is not unusual to find materials that have a large defect content. For example, ZrO_2 is often doped with 0.2 *mol fraction* yttrium for fuel cell applications,[15] which results in a highly defective crystalline lattice that contains a large number of aliovalent substitutional yttrium ions as well as their charge-compensating oxygen vacancies.[16–18] Indeed it has been recognized that there are strong scientific as well as technological incentives to develop a defect theory that has general applicability, even in the high-defect-concentration regime. In order to accomplish this objective, however, it is necessary to first identify the causes that lead to the break down of the traditional theory.

It is clear that in the case of high defect concentrations, more defects are crowded together. The Coulombic interactions among the charged species then become stronger and can no longer be adequately approximated by the Debye-Hückel correction. In addition the spatial locations of the defects are no longer statistically uncorrelated because of the exclusion effect, in which the presence of a defect excludes others from occupying or sharing the same region in the lattice. A general defect theory thus needs to account for these two effects: interactions and exclusions.

In the past decades a number of formalisms have been

0163-1829/94/49(2)/864(17)/$06.00 ©1994 The American Physical Society

proposed to treat high-concentration point-defect chemistry. Rau studied the defect chemistry of Cu_2S as functions of T and P_{S_2} using a set of modified mass action equations.[19] These equations are corrected for the exclusion effect by directly subtracting the sites already occupied by existing defects from the total number of lattice sites. This approach, however, does not account for the effect of defect interactions. Its treatment of the exclusion effect is also too simplistic.

Libowitz studied the sulfide[20] and hydride systems[21,22] using an approach similar to that of the Ising-Langmuir-type thermodynamic functions.[23,24] Here the defects are assumed to be randomly distributed, and only those that happen to be nearest neighbors contribute a fixed amount of energy to the total system Gibbs free energy. Fong made further refinement with the inclusion of the Debye-Hückel correction.[25] This approach, nevertheless, does not provide a configurational entropy that properly accounts for the defect exclusion effect, neither does it properly account for the long-range Coulombic interaction effect.

Atlas introduced the "spacing statistics" to treat nonstoichiometric fluorite structured oxide systems.[26–28] This formalism had been reviewed by Manes.[29] In this approach a mathematical "spacing rule" is used to divide the lattice into space-filling subzones, such that each of these zones contains exactly one oxygen vacancy. A subzone of the ith spacing level then encloses C_i lattice sites and corresponds to a specific energy level. An overall partition function is obtained based on the energetic contributions of all the subzones. This formulation has been used to calculate various thermodynamic quantities as functions of vacancy concentrations. It, however, does not describe the relationships between defect concentrations and environmental parameters such as P_{O_2}, and is difficult to be extended to situations in which multiple defect species are present. In addition, this methodology appears to have used an incorrect expression for the configurational entropy S_{conf} which is derived from Ω, the number of ways to arrange all the subzones in the lattice:[29]

$$\Omega = \prod_{i=0,L} C_i^{n_i} \frac{\omega_i!}{(\omega_i - n_i)! n_i!} ,$$
$$\omega_i = \frac{(B + n_i C_i - \sum_{r=0,i} n_r C_r)}{C_i} , \tag{1}$$

where B is the total number of oxide ion lattice sites, n_i is the number of subzones of the ith level, ω_i is the lattice space (normalized to C_i) available to n_i, C_i is one level larger in size than C_{i+1} and $\prod_{i=0,L}$ multiplies over all the $(L+1)$ spacing levels. It is noted that Ω_i is obtained based on a process in which the largest subzones are placed into the lattice first, followed by the next smaller subzones, and so on down to the smallest subzones. In this way the ω_i expression is acquired by subtracting from B the lattice space that is already occupied by subzones that are *larger* than C_i. Hence the $\sum_{r=0,i}$ term. This expression is nevertheless unsymmetric with respect to subzones of different sizes, which suggests that the value of S_{conf} $(=k_B \ln\Omega)$ *depends* on the order in which the different sized subzones are placed into the lattice. Since a proper thermodynamic state function, such as entropy, should be independent of the path taken in the calculation, it is clear that Ω as defined in Eq. (1) does not give the correct S_{conf}.

This work describes a defect chemistry formalism of general applicability in inorganic crystalline solids. The focus of this approach is an expression for the virtual chemical potential of point defect. This expression is derived by considering a system Gibbs free energy that incorporates both the short-range as well as the long-range Coulombic defect interactions, and a configurational entropy that incorporates the generalized defect exclusions. The defect chemistry can then be established in a manner similar to that of the traditional approach, in which the chemical potentials of different species and the environment are balanced, as required under thermodynamic equilibrium conditions, to arrive at a set of equations that govern defect concentrations. The applicability of this formulation is demonstrated in two ways. Firstly it is shown that, at the limit of low defect concentrations, the current formulation is equivalent to the traditional defect chemistry formulation. Secondly a detailed example is worked out to study the defect chemistry of nonstoichiometric $CeO_{2-\delta}$ (δ is the oxygen deficiency) as functions of T and P_{O_2}. The defect concentrations are calculated using a numerical routine based on the conjugate gradient algorithm,[30] which is briefly described in the Appendix. In the example, the oxygen deficiency δ is obtained as the net concentrations of all oxygen-vacancy-containing defect species, and the results are compared with literature data. The effects of defect interactions and exclusions are examined, and the defect thermodynamic activities are calculated as functions of environmental parameters.

The undoped ionic $CeO_{2-\delta}$ is selected here because it is a well studied system. Its lattice can sustain high degree of nonstoichiometry over a large range of P_{O_2} without undergoing a phase change.[31–33] Under reducing atmosphere it is oxygen deficient and contains several point defect species.[14,34–36] It should be emphasized that the intent of this work is to develop a general defect chemistry formalism that is applicable even in the high-defect-concentration regime, but not to study the point-defect chemistry of the CeO_2 system, which is a well researched topic.[14,31–40]

II. BASIC FORMULATION

In this section the system Gibbs free energy G is derived as a function of point-defect concentrations. This is carried out with the incorporation of defect interaction and exclusion effects. The fluorite structured CeO_2 (Ref. 41) is used as a model system. It is known that the defect chemistry of the oxygen deficient $CeO_{2-\delta}$ in the P_{O_2} range of interest may be described using five different point-defect species:[34–36] the reduced cerium ion Ce'_{Ce}; two types of oxygen vacancies at different charge states,

$V_O^{\cdot\cdot}$ and $V_O^{\cdot}$; and two types of defect pairs formed by the association of Ce'_{Ce} with the appropriate oxygen vacancies, $(CeV_O)^{\cdot}$ and $(CeV_O)^{\times}$. (Note that in this paper the phrase "point defect" is used loosely and refers to both simple defects that occupy only a single lattice site, as well as defect complexes that are formed by the association of more than one simple defects.) Also present in the lattice are the host cations $Ce_{Ce}^{\times}$, and host anions $O_O^{\times}$. The point defects are denoted by the Kröger-Vink notation,[4,5] in which the main letter identifies the defect species, the subscript gives the lattice location, and the superscript gives the effective charge with respect to the perfect lattice ("$\cdot$" $=+|e|$, "$'$"$=-|e|$, and "$\times$"$=0$, where $|e|$ is the electronic charge). Henceforth in this paper, unless otherwise specified, the word "charge" refers to the effective charge. Here it is interesting to note that Ce'_{Ce} is often thought of as formed by an electron polaron sitting on a $Ce_{Ce}^{\times}$.[34,36,42,43] Figure 1 shows schematically a planner projection of the CeO_2 lattice containing the above-mentioned defect species.

Let us now consider a perfect CeO_2 lattice that has N_c cation sites and N_a anion sites, such that $N_a=2N_c$ from structural consideration. The introduction of point defects into this otherwise perfect lattice results in a change in the system Gibbs free energy. This is expressed below with the configurational entropy term separated out explicitly:[6,7,44]

$$G=\sum_\alpha n_\alpha\langle g_\alpha\rangle - TS_{\text{conf}}$$
$$=G^*-k_BT\ln\Omega\ , \tag{2}$$

where n_α is the number of α-type defect that has mean free energy of formation $\langle g_\alpha\rangle$, $\sum_\alpha$ sums over all species, Ω is the number of ways that all these defects can be arranged in the lattice, $S_{\text{conf}}=k_B\ln\Omega$ is the configurational entropy, and k_B and T have their usual meanings. Notice that $\langle g_\alpha\rangle$ here still contains nonconfigurational component of the formation entropy.

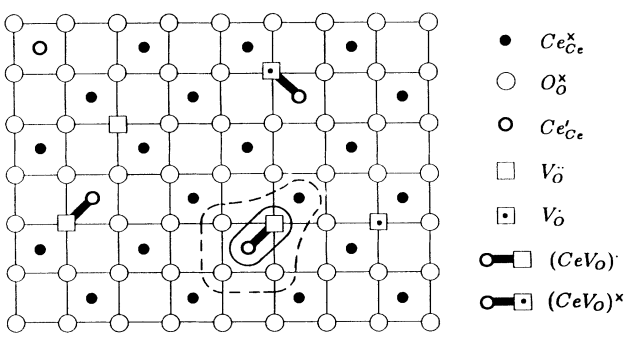

FIG. 1. Planner projection of the fluorite structure of a CeO_2 lattice that contains various species of point defects and defect complexes. The envelopes show two different possible ways of defining the extent of the short-range interaction due to the $(CeV_O)^{\cdot}$ pair. Region I is inside the envelope, and region II is the rest of the lattice.

A. Free energy of formation of a single defect

The formation free energy of a defect is commonly thought of as having contributions from two classes of interactions.[45,46] The first class is the short-range interactions between the defect and its neighboring ions such as the Lennard-Jones-type force.[46,47] In general, the strength of this class of interactions is considered to be negligible except in the immediate vicinity of the defect. This can be seen from the fact that these interactions are partly responsible for the local lattice distortion, which typically has a strain field that falls off rapidly as $1/r^3$ (Ref. 48) (r is the distance) such that the displacement of the lattice ions become negligible beyond the nearest neighbors.[49] The second class is the Coulombic interaction between charged defects. This interaction has very long range because its associated potential field falls off relatively slowly as $1/r$.[50] It should be noted that the host lattice ions, because of their neutral charge states, do not take part in the Coulombic interaction.

Let us now draw an envelope about a defect that defines the extent of the associated short-range interactions. Inside this envelope is region I and outside it is region II. Figure 1 shows two possible choices of such envelopes that enclose a $(CeV_O)^{\cdot}$ pair. The outer dash-line envelope encloses all the nearest-neighbor sites to this defect. The inner solid-line envelope, on the other hand, contains only the sites occupied by the defect itself. The latter case, while rather simplistic, turns out to be a convenient choice for the calculation purpose, and is the choice used in this work.

As a result of the definition of the envelope, the formation free energy g_α may now be written as having two components:

$$g_\alpha=g_\alpha^{\text{I}}+g_\alpha^{\text{II}}\ . \tag{3}$$

Here g_α^{I} includes all the contributions due to interactions inside the envelope. Note that this includes *both* the short-range and the Coulombic interactions. On the other hand, g_α^{II} essentially contains only contributions from the Coulombic interactions between the reference defect and all other charged defects present in the rest of the lattice. This is because the strength of the short-range interactions are negligible in region II.

Since g_α^{I} does not have any contribution from outside the envelope, its value depends only on the defect and the lattice structures inside the envelope. As a result it may be considered to be a constant that is independent of defect concentrations. The same, however, cannot be said of g_α^{II}, which is clearly a strong function of defect concentrations because of the contributions from interaction with all the other defects in the lattice. Since g_α^{II} is expected to approach zero when there are very few defects, Eq. (3) then suggests that $g_\alpha\cong g_\alpha^{\text{I}}$ in the limit of low defect concentrations. Thus in principle g_α^{I} may be determined experimentally by measuring g_α under carefully controlled conditions of low defect concentrations. It may also be obtained using well established computer codes such as HADES (Refs. 51–53) or CASCADE (Refs. 54–59) whose applicabilities have been demonstrated in previous work on various ionic systems including the

fluorite structured oxides. In the case where there is a significant electronic contribution g_α^{I} may be calculated using the ICECAP code.[60]

In order to evaluate g_α^{II} it is noted that all defects may be thought of as being made up of a few basic "building-block species," each of which is a simple defect occupying a single lattice site. These building-block species may be further classified into the cationic type that sits on the cation sites, and the anionic type that sits on the anion sites. In general, any defect may be thought of as consisting m_c cationic building-block defects, and m_a anionic ones. Using this concept, all the point defects shown in Fig. 1 may be constructed with just three building-block species: $\mathrm{Ce}'_{\mathrm{Ce}}$, $V_{\mathrm{O}}^{\cdot\cdot}$, and $V_{\mathrm{O}}^{\cdot}$. For example, $\mathrm{Ce}'_{\mathrm{Ce}}$ is made up of $m_c=1$ cationic $\mathrm{Ce}'_{\mathrm{Ce}}$ and no anionic building-block defect, whereas $(\mathrm{CeV_O})^{\cdot}$ is made up of $m_c=1$ cationic $\mathrm{Ce}'_{\mathrm{Ce}}$ and $m_a=1$ anionic $V_{\mathrm{O}}^{\cdot\cdot}$. Consequently a g_α^{II} expression can be written by summing over the Coulombic interactions between the constituent building-block defects and all the other defects (also considered as made up of building-block defects) outside the envelope:

$$4\pi\varepsilon_r\varepsilon_0 g_\alpha^{\mathrm{II}} = \sum_{\beta_c=1,m_c} Q_{\beta_c}(a_{\beta_c})\left[\sum_{j\notin I}\frac{Q(j)}{R_{a_{\beta_c}j}}\right] + \sum_{\beta_a=1,m_a} Q_{\beta_a}(a_{\beta_a})\left[\sum_{j\notin I}\frac{Q(j)}{R_{a_{\beta_a}j}}\right], \quad (4)$$

where $\sum_{\beta_c}=1,m_c$ sums over all the m_c cationic building-block defects inside the envelope, a_{β_c} denotes their respective lattice locations, $Q_{\beta_c}(a_{\beta_c})$ denotes their respective charges, and $\sum_{\beta_a}=1,m_a$, a_{β_a}, and $Q_{\beta_a}(a_{\beta_a})$ have similar meanings for the anionic building-block defects. Here $\sum_{j\notin I}$ sums over all lattice sites outside the envelope ($j\notin I$ indicates that j site is not inside region I defined by the envelope), $Q(j)$ is the charge at site j, $R_{a_\beta j}$ is the distance between sites a_β and j, and ε_r and ε_0 are the relative dielectric constant and the permittivity of free space, respectively. The first term on the right-hand side of Eq. (4) is the contribution from the cationic building-block defects, and the second term is that from the anionic ones. Note that here g_α^{II} does not have any contributions from the host ions or from the neutral building-block defects because they have $Q(j)=0$.

It should be noted that in this paper the defect charges are assumed to be point charges that are integral multiples of $|e|$. It is further assumed that the same charge is carried by a defect whether it is an isolated defect or acts as a building-block of a defect complex. In other words, an isolated $V_{\mathrm{O}}^{\cdot}$ and the constituent vacancy in $(\mathrm{Ce}V_{\mathrm{O}})^{\times}$ are both assumed to carry the same charge of $+|e|$. Strictly speaking this assumption may not be correct. It is known, for example, that $V_{\mathrm{O}}^{\cdot}$ may be formed by an electron trapped in an oxygen vacancy. The captured electron does not stay on the vacated anion lattice site, but is instead delocalized and distributed among the surrounding cations.[46] As a result, it is conceivable that $V_{\mathrm{O}}^{\cdot}$ and its surrounding cations may all carry fractional and distributed charges. This electron distribution may be further distorted in the case of $(\mathrm{Ce}V_{\mathrm{O}})^{\times}$ when there is a $\mathrm{Ce}'_{\mathrm{Ce}}$ sitting right next to $V_{\mathrm{O}}^{\cdot}$.

In addition, it is recognized that the present formulation may require further modification in order to account for the effect of polarization,[47,48] which can have significant contribution to the defect formation and interaction energies. In the current frame work, the polarization energy may be included as a constant and integral component of g_α^{I}. This component, however, may have a range that extends beyond region I. This definition, while workable in the dilute limit, is nevertheless unsatisfactory at higher defect concentrations, at which point the defect interactions can cause non-negligible changes in the polarization energy. In the case of g_α^{II}, an attempt is already made in this work to account for the polarization effect by incorporating ε_r into the calculation of the Coulombic interaction energy [for example, see Eq. (4)].

The above-mentioned complications due to the distributed charges and the ionic polarization, however, are beyond the scope of the current paper. It is the author's opinion that the inclusion of these effects would not significantly alter the conclusions of this paper.

B. Mean free energy of formation

The mean value of g_α may be obtained by averaging over all α-type defects:

$$\langle g_\alpha\rangle = \langle g_\alpha^{\mathrm{I}}\rangle + \langle g_\alpha^{\mathrm{II}}\rangle , \quad (5)$$

where $\langle\ \rangle$ indicates a mean quantity. Since g_α^{I} depends only on the structure inside the envelope, which is the same for all α defects, one has

$$\langle g_\alpha^{\mathrm{I}}\rangle = g_\alpha^{\mathrm{I}} . \quad (6)$$

Furthermore, all α defects contain the same constituent building-block defects. Consequently one obtains from Eq. (4):

$$4\pi\varepsilon_r\varepsilon_0\langle g_\alpha^{\mathrm{II}}\rangle = \sum_{\beta_c=1,m_c} Q_{\beta_c}(a_{\beta_c})\left[\sum_{j\neq a_{\beta_c}}^{\text{all sites}}\frac{\langle Q(j)\rangle}{R_{a_{\beta_c}j}} - \sum_{j\in I;j\neq a_{\beta_c}}\frac{\langle Q(j)\rangle}{R_{a_{\beta_c}j}}\right] + \sum_{\beta_a=1,m_a} Q_{\beta_a}(a_{\beta_a})\left[\sum_{j\neq a_{\beta_a}}^{\text{all sites}}\frac{\langle Q(j)\rangle}{R_{a_{\beta_a}j}} - \sum_{j\in I;j\neq a_{\beta_a}}\frac{\langle Q(j)\rangle}{R_{a_{\beta_a}j}}\right], \quad (7)$$

where $\langle Q(j)\rangle$ is the mean charge at site j. Here each of the $\sum_j$ terms on the right-hand side of Eq. (4) has been extended into the envelope by appropriately compensating for the additional contributions. Thus the $\sum_{j\in I}$ terms sum over only those sites inside the envelope, and the $\sum_{j\neq a_\beta}^{\text{all sites}}$ terms sum over the whole lattice except site a_β. Note that in Eq. (7) the region I contributions always cancel each other out as long as the same lattice is consistently used inside the envelope. Thus any region I lattice may be used in this calculation. It is thus convenient to assume a perfect lattice inside the envelope. This also allows one to avoid the difficulty of not knowing the actual lattice structure inside the envelope, which may be highly distorted by the presence of defect.

It turns out that $\langle Q(j)\rangle$ in Eq. (7) can have only one of two different values. It can either be the mean charge at the cation site $\langle Q_c\rangle$, or that at the anion site $\langle Q_a\rangle$. These $\langle Q\rangle$ values are constants that may be obtained by averaging the charges of all building-block defects over the respective sublattices. One can then further divide each of the right-hand side terms in Eq. (7) into two parts that sum over, respectively, the cation and the anion sublattices:

$$\begin{aligned}4\pi\varepsilon_r\varepsilon_0\langle g_\alpha^{\mathrm{II}}\rangle = &\sum_{\beta_c=1,m_c} Q_{\beta_c}(a_{\beta_c})\left[\langle Q_c\rangle \sum_{j_c\neq a_{\beta_c}}^{\text{cation sites}} \frac{1}{R_{a_{\beta_c}j_c}} + \langle Q_a\rangle \sum_{j_a}^{\text{anion sites}} \frac{1}{R_{a_{\beta_c}j_a}}\right]\\ &-\sum_{\beta_c=1,m_c} Q_{\beta_c}(a_{\beta_c})\left[\langle Q_c\rangle \sum_{j_c\in I;j_c\neq a_{\beta_c}}^{\text{cation sites}} \frac{1}{R_{a_{\beta_c}j_c}} + \langle Q_a\rangle \sum_{j_a\in I}^{\text{anion sites}} \frac{1}{R_{a_{\beta c}j_a}}\right]\\ &+\sum_{\beta_a=1,m_a} Q_{\beta_a}(a_{\beta_a})\left[\langle Q_c\rangle \sum_{j_c}^{\text{cation sites}} \frac{1}{R_{a_{\beta_a}j_c}} + \langle Q_a\rangle \sum_{j_a\neq a_{\beta_a}}^{\text{anion sites}} \frac{1}{R_{a_{\beta_a}j_a}}\right]\\ &-\sum_{\beta_a=1,m_a} Q_{\beta_a}(a_{\beta_a})\left[\langle Q_c\rangle \sum_{j_c\in I}^{\text{cation sites}} \frac{1}{R_{a_{\beta_c}j_c}} + \langle Q_a\rangle \sum_{j_a\in I;j_a\neq a_{\beta_a}}^{\text{anion sites}} \frac{1}{R_{a_{\beta_a}j_a}}\right].\end{aligned} \tag{8}$$

From the overall charge neutrality condition one has

$$\langle Q_c\rangle + 2\langle Q_a\rangle = 0\ . \tag{9}$$

Substituting Eq. (9) into Eq. (8):

$$\begin{aligned}4\pi\varepsilon_r\varepsilon_0\langle g_\alpha^{\mathrm{II}}\rangle = \langle Q_c\rangle \Bigg\{ &\sum_{\beta_c=1,m_c} Q_{\beta_c}(a_{\beta_c})\left[\sum_{j_c\neq a_{\beta_c}}^{\text{cation sites}} \frac{1}{R_{a_{\beta_c}j_c}} - \frac{1}{2}\sum_{j_a}^{\text{anion sites}} \frac{1}{R_{a_{\beta_c}j_a}}\right]\\ &+\sum_{\beta_a=1,m_a} Q_{\beta_a}(a_{\beta_a})\left[\sum_{j_c}^{\text{cation sites}} \frac{1}{R_{a_{\beta_a}j_c}} - \frac{1}{2}\sum_{j_a\neq a_{\beta_a}}^{\text{anion sites}} \frac{1}{R_{a_{\beta_a}j_a}}\right.\\ &-\sum_{\beta_c=1,m_c} Q_{\beta_c}(a_{\beta_c})\left[\sum_{j_c\in I;j_c\neq a_{\beta_c}}^{\text{cation sites}} \frac{1}{R_{a_{\beta_c}j_c}} - \frac{1}{2}\sum_{j_a\in I}^{\text{anion sites}} \frac{1}{R_{a_{\beta_c}j_a}}\right]\\ &-\sum_{\beta_a=1,m_a} Q_{\beta_a}(a_{\beta_a})\left[\sum_{j_c\in I}^{\text{cation sites}} \frac{1}{R_{a_{\beta_a}j_c}} - \frac{1}{2}\sum_{j_a\in I;j_a\neq a_{\beta_a}}^{\text{anion sites}} \frac{1}{R_{a_{\beta_a}j_a}}\right]\Bigg\}.\end{aligned} \tag{10}$$

Equation (10) now can be simplified using the Madelung constants.[46] Let us first write down the Coulombic energy U due to the interactions between the real charge of a reference host Ce^{4+} cation (i.e., $Ce_{Ce}^{\times}$) and the real charges of all the other ions in a perfect CeO_2 lattice:

$$4\pi\varepsilon_r\varepsilon_0 U = q_c \left[\sum_{j_c \neq a_{\beta_c}}^{\text{cation sites}} \frac{q_c}{R_{a_{\beta_c} j_c}} + \sum_{j_a}^{\text{anion sites}} \frac{q_a}{R_{a_{\beta_c} j_a}} \right]$$

$$= q_c \left\{ q_c \left[\sum_{j_c \neq a_{\beta_c}}^{\text{cation sites}} \frac{1}{R_{a_{\beta_c} j_c}} - \frac{1}{2} \sum_{j_a}^{\text{anion sites}} \frac{1}{R_{a_{\beta_c} j_a}} \right] \right\}$$

$$= q_c M_c \ , \tag{11}$$

where M_c is the Madelung constant associated with the reference Ce^{4+} cation located at a_{β_c} site, and $q_c = +4|e|$, $q_a = -2|e|$ are the real charges carried by the Ce^{4+} and O^{2-} host ions, respectively. Here the overall neutrality requirement for the real charges, $q_c + 2q_a = 0$, has been used in the derivation of Eq. (11). In a similar manner one may write down the Coulombic energy of a reference host O^{2-} anion (i.e., $O_O^{\times}$) located at a_{β_a} site, from which the associated Madelung constant may be found to be

$$M_a = q_c \left[\sum_{j_c}^{\text{cation sites}} \frac{1}{R_{a_{\beta_a} j_c}} - \frac{1}{2} \sum_{j_a \neq a_{\beta_a}}^{\text{anion sites}} \frac{1}{R_{a_{\beta_a} j_a}} \right] . \tag{12}$$

Note that it is again assumed here that all the ions are point charges. For delocalized charges, one may need to use the Ewald procedure[61] to calculate the Madelung constants instead of using the expressions given in Eqs. (11) and (12).

Substituting the expressions of the Madelung constants in Eqs. (11) and (12) back into Eq. (10) one then obtains

$$\langle g_\alpha^{\text{II}} \rangle = \frac{\mathcal{L}_\alpha}{4\pi\varepsilon_r\varepsilon_0} \langle Q_c \rangle \ , \tag{13}$$

where $\mathcal{L}_\alpha$ is a function whose value depends only on the structure inside region I. It is given by

$$\mathcal{L}_\alpha = \frac{M_c}{q_c} \sum_{\beta_c = 1, m_c} Q_{\beta_c}(a_{\beta_c}) + \frac{M_a}{q_a} \sum_{\beta_a = 1, m_a} Q_{\beta_a}(a_{\beta_a}) - \sum_{\beta_c = 1, m_c} Q_{\beta_c}(a_{\beta_c}) \left[\sum_{j_c \in I; j_c \neq a_{\beta_c}}^{\text{cation sites}} \frac{1}{R_{a_{\beta_c} j_c}} - \frac{1}{2} \sum_{j_a \in I}^{\text{anion sites}} \frac{1}{R_{a_{\beta_c} j_a}} \right]$$

$$- \sum_{\beta_a = 1, m_a} Q_{\beta_a}(a_{\beta_a}) \left[\sum_{j_c \in I}^{\text{cation sites}} \frac{1}{R_{a_{\beta_c} j_c}} - \frac{1}{2} \sum_{j_a \in I; j_a \neq a_{\beta_a}}^{\text{anion sites}} \frac{1}{R_{a_{\beta_c} j_a}} \right] . \tag{14}$$

Here $\mathcal{L}_\alpha$ can be viewed as a measure of the strength of the Coulombic force on the α species. Combining Eqs. (5), (6), and (13), the mean free energy of formation per α defect is obtained:

$$\langle g_\alpha \rangle = g_\alpha^{\text{I}} + \frac{\mathcal{L}_\alpha}{4\pi\varepsilon_r\varepsilon_0} \langle Q_c \rangle \ . \tag{15}$$

Notice that g_α^{I}, $\mathcal{L}_\alpha$ are both constants whose values depend on the characteristics of the α species only. Thus the concentration dependence information of $\langle g_\alpha \rangle$ is all contained in $\langle Q_c \rangle$.

C. Configurational entropy

The configurational entropy as defined in Eq. (2) is given by $S_{\text{conf}} = k_B \ln\Omega$, where Ω is the total number of ways that all defects may be arranged in the lattice. This may be written as

$$\ln\Omega = \sum_\alpha \ln\Omega_\alpha \ , \tag{16}$$

where Ω_α is the number of ways that n_α α defects may be arranged in a lattice that *already* contains all the non-α-type defects, $\sum_\alpha$ sums over all defect species.

Let us first consider the introduction of a single α defect into a lattice that already contains many different defects, which may include some α defects. Let B_α be the total number of ways that an α defect may be arranged in a perfect lattice. One may find that each of the preexisting defects makes several of the B_α ways no longer possible. In other words, several of the B_α ways have been "excluded" from taking place. One can thus define an "exclusion factor" $\Lambda_{\alpha,\beta}$, which is the number of ways of placing an α defect in a perfect lattice that is being excluded due to the presence of a single β defect. This concept is schematically illustrated in Fig. 2 for the case of $\alpha = (CeV_O)^{\cdot}$. Here each of the envelopes represents an "exclusion zone" that has been denied to $(CeV_O)^{\cdot}$ due to a preexisting β defect. It can be seen that about Ce'_{Ce} there are Z_c such exclusion zones, where $Z_c = 8$ is the coordination number of $O_O^{\times}$ sites about a $Ce_{Ce}^{\times}$ site.[41] Each one of these envelopes encloses both the Ce'_{Ce} and one of its nearest neighboring $O_O^{\times}$ site. As a result there are a total of $\Lambda_{(CeV_O)^{\cdot}, Ce'_{Ce}} = Z_c$ ways of arranging $(CeV_O)^{\cdot}$

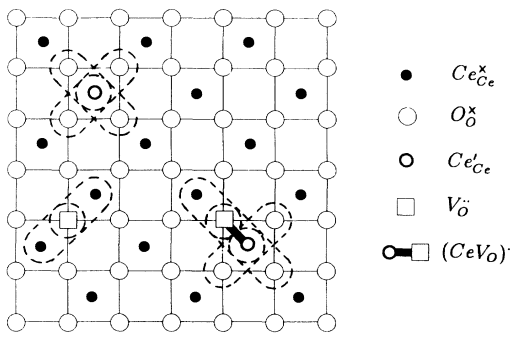

FIG. 2. Planner projection of the CeO_2 lattice. Each dashed envelope indicate one way of arranging the $(CeV_O)^{\cdot}$ pair that is being excluded by the preexisting defects.

that is being excluded because of the presence of a single Ce'_{Ce}. From Fig. 2 it can also be seen that $\Lambda_{(CeV_O)^{\cdot},V_O^{\cdot\cdot}}=Z_a$ where $Z_a=4$ is the coordination number of $Ce_{Ce}^{\times}$ about $O_O^{\times}$,[41] and that $\Lambda_{(CeV_O)^{\cdot},(CeV_O)^{\cdot}}=(Z_c+Z_a-1)$. The values of $\Lambda_{\alpha,\beta}$ for all the possible (α,β) combinations are listed in Table I. It is interesting to note that the approach taken in this work focuses on the concept of generalized exclusion in which it is the *ways* of placing defects that are being excluded, rather than the traditional concept in which it is the *sites* that are being excluded.[19,26–28,62]

Taking into consideration the generalized exclusion effect described above, the number of ways to arrange n_α α defects then becomes

$$\Omega_\alpha=\frac{\left[B_\alpha+\Lambda_{\alpha,\alpha}n_\alpha-\sum_\beta\Lambda_{\alpha,\beta}n_\beta\right]!}{n_\alpha!\left[B_\alpha+(\Lambda_{\alpha,\alpha}-1)n_\alpha-\sum_\beta\Lambda_{\alpha,\beta}n_\beta\right]!}\ . \tag{17}$$

Using Sterling's approximation, one obtains

$$\begin{aligned}\ln\Omega_\alpha\cong&\left[B_\alpha+\Lambda_{\alpha,\alpha}n_\alpha-\sum_\beta\Lambda_{\alpha,\beta}n_\beta\right]\\&\times\ln\left[B_\alpha+\Lambda_{\alpha,\alpha}n_\alpha-\sum_\beta\Lambda_{\alpha,\beta}n_\beta\right]-n_\alpha\ln n_\alpha\\&-\left[B_\alpha+(\Lambda_{\alpha,\alpha}-1)n_\alpha-\sum_\beta\Lambda_{\alpha,\beta}n_\beta\right]\\&\times\ln\left[B_\alpha+(\Lambda_{\alpha,\alpha}-1)n_\alpha-\sum_\beta\Lambda_{\alpha,\beta}n_\beta\right]\ .\end{aligned} \tag{18}$$

It is then possible to obtain the configurational entropy by substituting Eqs. (16) and (18) into the $S_{\rm conf}$ definition of Eq. (2).

It is interesting to compare the Ω_α in Eq. (17) with the Ω of the spacing statistics in Eq. (1). It can be seen that the Ω_α expression here is symmetric with respect to the different defect species. In other words one can always obtain the same $S_{\rm conf}=k_B\ln\Omega$ regardless of the order in which the different defect species are placed in the lattice.

III. VIRTUAL CHEMICAL POTENTIAL OF POINT DEFECT

The virtual chemical potential of the α-species point defect is defined as:[63,64]

$$\mu_\alpha=\frac{\partial G}{\partial n_\alpha}\ . \tag{19}$$

It is worth noting that μ_α is called the "virtual chemical potential" instead of "chemical potential" because the partial derivative in Eq. (19) requires that the numbers of all other species be fixed while n_α is varied. As Guggenheim has pointed out,[63] this condition cannot be satisfied because the defect concentrations are not independent quantities due to the charge neutrality constraint. In other words, it is impossible to, say, remove a positively charged defect without also decreasing the number of some negatively charged defects. Consequently, μ_α given in Eq. (19) cannot be measured experimentally, but can nevertheless be viewed as a mathematical device that facilitates theoretical derivations and calculations. In defect chemistry formulation this charge imbalance problem is customarily addressed by imposing an additional constraint that requires overall charge neutrality.

Combining Eqs. (2), (16), and (19), one has

$$\mu_\alpha=\mu_\alpha^*-k_BT\sum_\beta\frac{\partial\ln\Omega_\beta}{\partial n_\alpha}\ , \tag{20}$$

where

$$\mu_\alpha^*=\frac{\partial G^*}{\partial n_\alpha}\ . \tag{21}$$

Here μ_α^* may be obtained by combining Eq. (21) with the definition of G^* in Eq. (2) and the $\langle g_\alpha\rangle$ expression in Eq. (15):

TABLE I. The parameters used in the defect chemistry calculations in nonstoichiometric $CeO_{2-\delta}$ system, including $\Lambda_{\alpha,\beta}$, y_α, $x_\alpha^{\max}$, and $\mathcal{L}_\alpha$. $Z_c=8$, $Z_a=4$, $M_c=-2.62\times10^{-9}$ C/m, $M_a=4.27\times10^{-9}$ C/m, and $l_0=a_0/2=2.706$ Å (Ref. 41).

		β							
	$\Lambda_{\alpha,\beta}$	Ce'_{Ce}	$V_O^{\cdot\cdot}$	$V_O^{\cdot}$	$(CeV_O)^{\cdot}$	$(CeV_O)^{\times}$	y_α	$x_\alpha^{\max}$	$\mathcal{L}_\alpha$
	Ce'_{Ce}	1	0	0	1	1	1	1	$-M_c/4$
	$V_O^{\cdot\cdot}$	0	1	1	1	1	2	2	$-M_a$
α	$V_O^{\cdot}$	0	1	1	1	1	2	2	$-M_a/2$
	$(CeV_O)^{\cdot}$	Z_c	Z_a	Z_a	Z_c+Z_a-1	Z_c+Z_a-1	Z_c	1	$-M_c/4-M_a-5\lvert e\rvert/2l_0$
	$(CeV_O)^{\times}$	Z_c	Z_a	Z_a	Z_c+Z_a-1	Z_c+Z_a-1	Z_c	1	$-M_c/4-M_a/2-3\lvert e\rvert/2l_0$

$$\mu_\alpha^* = g_\alpha^{\mathrm{I}} + \frac{1}{4\pi\varepsilon_r\varepsilon_0}\left[\mathcal{L}_\alpha\langle Q_c\rangle + \left[\sum_\beta \mathcal{L}_\beta n_\beta\right]\frac{\partial\langle Q_c\rangle}{\partial n_\alpha}\right] . \tag{22}$$

Differentiating Eq. (18) with respect to n_α:

$$\frac{\partial \ln\Omega_\beta}{\partial n_\alpha} = \delta_{\alpha\beta}\ln\frac{B_\beta + (\Lambda_{\beta,\beta}-1)n_\beta - \sum_\gamma \Lambda_{\beta,\gamma}n_\gamma}{n_\beta} + (\delta_{\alpha\beta}\Lambda_{\beta,\beta} - \Lambda_{\beta,\alpha}) \times \ln\frac{B_\beta + \Lambda_{\beta,\beta}n_\beta - \sum_\gamma \Lambda_{\beta,\gamma}n_\gamma}{B_\beta + (\Lambda_{\beta,\beta}-1)n_\beta - \sum_\gamma \Lambda_{\beta,\gamma}n_\gamma} , \tag{23}$$

where $\delta_{\alpha\beta}$ is the Kronecker delta function. Summing over all defect species one gets

$$\sum_\beta \frac{\partial \ln\Omega_\beta}{\partial n_\alpha} = \ln\frac{B_\alpha + (\Lambda_{\alpha,\alpha}-1)n_\alpha - \sum_\beta \Lambda_{\alpha,\beta}n_\beta}{n_\alpha} + \Lambda_{\alpha,\alpha}\ln\frac{B_\alpha + \Lambda_{\alpha,\alpha}n_\alpha - \sum_\beta \Lambda_{\alpha,\beta}n_\beta}{B_\alpha + (\Lambda_{\alpha,\alpha}-1)n_\alpha - \sum_\beta \Lambda_{\alpha,\beta}n_\beta} - \sum_\gamma \Lambda_{\gamma,\alpha}\ln\frac{B_\gamma + \Lambda_{\gamma,\gamma}n_\gamma - \sum_\beta \Lambda_{\gamma,\beta}n_\beta}{B_\gamma + (\Lambda_{\gamma,\gamma}-1)n_\gamma - \sum_\beta \Lambda_{\gamma,\beta}n_\beta} . \tag{24}$$

Let us define the normalized defect concentration, x_α:

$$x_\alpha = \frac{n_\alpha}{N_c} . \tag{25}$$

It is noted that B_α is in general an integral multiple of the total number of cation sites N_c, hence it is convenient to define the normalized quantity

$$y_\alpha = \frac{B_\alpha}{N_c} . \tag{26}$$

The y_α values of different defect species are listed in Table I. One can then rewrite Eqs. (22) and (24) in terms of x_α and y_α:

$$\mu_\alpha^* = g_\alpha^{\mathrm{I}} + \frac{1}{4\pi\varepsilon_r\varepsilon_0}\left[\mathcal{L}_\alpha\langle Q_c\rangle + \left[\sum_\beta \mathcal{L}_\beta x_\beta\right]\frac{\partial\langle Q_c\rangle}{\partial x_\alpha}\right] , \tag{27}$$

$$\sum_\beta \frac{\partial \ln\Omega_\beta}{\partial n_\alpha} = \ln\left[\frac{\mathcal{F}_\alpha}{x_\alpha}\right] , \tag{28}$$

where $\mathcal{F}_\alpha$ is a function of x_α given by

$$\ln\mathcal{F}_\alpha = \ln\left[y_\alpha + (\Lambda_{\alpha,\alpha}-1)x_\alpha - \sum_\beta \Lambda_{\alpha,\beta}x_\beta\right] + \Lambda_{\alpha,\alpha}\ln\left[\frac{y_\alpha + \Lambda_{\alpha,\alpha}x_\alpha - \sum_\beta \Lambda_{\alpha,\beta}x_\beta}{y_\alpha + (\Lambda_{\alpha,\alpha}-1)x_\alpha - \sum_\beta \Lambda_{\alpha,\beta}x_\beta}\right] - \sum_\beta \Lambda_{\beta,\alpha}\ln\left[\frac{y_\beta + \Lambda_{\beta,\beta}x_\beta - \sum_\gamma \Lambda_{\beta,\gamma}x_\gamma}{y_\beta + (\Lambda_{\beta,\beta}-1)x_\beta - \sum_\gamma \Lambda_{\beta,\gamma}x_\gamma}\right] . \tag{29}$$

Note that $\Lambda_{\alpha,\beta} \neq \Lambda_{\beta,\alpha}$. In Eq. (29), $\mathcal{F}_\alpha$ can be viewed as a measure of the fraction of lattice space that is not excluded by the preexisting defects and hence is still available to the placement of α defects. Substituting Eq. (28) back into Eq. (20) an expression for the virtual chemical potential of point defect is obtained:

$$\mu_\alpha = \mu_\alpha^* + k_B T \ln\left[\frac{x_\alpha}{\mathcal{F}_\alpha}\right] . \tag{30}$$

Note that μ_α^* contains all the information on the interaction effect (including that of both the short-range and the long-range Coulombic interactions), whereas $\mathcal{F}_\alpha$ contains all the information on defect exclusion effect. As a consequence the μ_α expression shown in Eq. (30) allows one to turn these two effects on and off individually in order to study their separate effects.

It is interesting to note that traditionally chemical potential is formally expressed as:[65]

$$\mu_\alpha = \mu_{\alpha,0}(T,P) + k_B T \ln\alpha_\alpha , \tag{31}$$

where $\mu_{\alpha,0}(T,P)$ is a constant whose value is defined by the chemical potential of the α species in a reference state of well defined T and P, and $a_\alpha = \gamma_\alpha x_\alpha$ is the activity of α species. Here γ_α is the activity coefficient. Let us make the identification

$$\mu_{\alpha,0} = g_\alpha^{\mathrm{I}} . \tag{32}$$

Combining Eqs. (27), (30), and (32) one has

$$\mu_\alpha = \mu_{\alpha,0} + \delta\mu_\alpha^* + k_B T \ln\left[\frac{x_\alpha}{\mathcal{F}_\alpha}\right] = \mu_{\alpha,0} + k_B T \ln\left[\frac{x_\alpha}{\mathcal{F}_\alpha}\exp\left[\frac{\delta\mu_\alpha^*}{k_B T}\right]\right] , \tag{33}$$

where

$$\delta\mu_\alpha^* = \frac{1}{4\pi\varepsilon_r\varepsilon_0}\left[\mathcal{L}_\alpha\langle Q_c\rangle + \left[\sum_\beta \mathcal{L}_\beta x_\beta\right]\frac{\partial\langle Q_c\rangle}{\partial x_\alpha}\right] . \tag{34}$$

Here $\delta\mu_\alpha^*$ can be looked upon as the change in μ_α^* due to Coulombic interactions among the defects. This is equal to the change in the free energy required to form a α defect. An expression for the defect activity can then be ob-

tained by comparing Eqs. (31) and (33):

$$a_\alpha = \frac{x_\alpha}{\mathcal{F}_\alpha} \exp\left[\frac{\delta\mu_\alpha^*}{k_B T}\right] . \tag{35}$$

IV. APPLICATION TO NONSTOICHIOMETRIC CERIUM DIOXIDE

This section uses the expression for virtual chemical potential of point defects derived in the previous section to formulate equations that govern the equilibrium defect concentrations. This study is carried out using the undoped nonstoichiometric $CeO_{2-\delta}$ as a model system.

A. Equations governing defect concentrations

The reactions between the defects in $CeO_{2-\delta}$ may be described by the following quasichemical equations:

$$O_O^\times + 2Ce_{Ce}^\times \leftrightarrow \tfrac{1}{2}O_2 + V_O^{\cdot\cdot} + 2Ce'_{Ce} , \tag{36}$$

$$V_O^{\cdot} + Ce_{Ce}^\times \leftrightarrow V_O^{\cdot\cdot} + Ce'_{Ce} , \tag{37}$$

$$Ce'_{Ce} + V_O^{\cdot\cdot} \leftrightarrow (CeV_O)^{\cdot} , \tag{38}$$

$$Ce'_{Ce} + V_O^{\cdot} \leftrightarrow (CeV_O)^{\times} . \tag{39}$$

Equation (36) describes the formation of $V_O^{\cdot\cdot}$ and Ce'_{Ce} by the reaction of the solid with environmental oxygen; Eq. (37) describes the equilibrium reaction between oxygen vacancies of different charge states; Eqs. (38) and (39) are the reactions that form, respectively, $(CeV_O)^{\cdot}$ and $(CeV_O)^{\times}$ defect pairs. At thermodynamic equilibrium the sum of μ_α's on the left-hand side of each of reactions (36)–(39) is exactly equal to that on the right-hand side. Thus one has

$$\mu_{O_O^\times} + 2\mu_{Ce_{Ce}^\times} = \tfrac{1}{2}\mu_{O_2} + \mu_{V_O^{\cdot\cdot}} + 2\mu_{Ce'_{Ce}} , \tag{40}$$

$$\mu_{V_O^{\cdot}} + \mu_{Ce_{Ce}^\times} = \mu_{V_O^{\cdot\cdot}} + \mu_{Ce'_{Ce}} , \tag{41}$$

$$\mu_{V_O^{\cdot\cdot}} + \mu_{Ce'_{Ce}} = \mu_{(CeV_O)^{\cdot}} , \tag{42}$$

$$\mu_{V_O^{\cdot}} + \mu_{Ce'_{Ce}} = \mu_{(CeV_O)^{\times}} . \tag{43}$$

Here the subscripts of the μ's indicate the identity and the charge state of corresponding species, μ_{O_2} is the chemical potential of oxygen in the environment. From Raoult's law[7,64] one has

$$\mu_{Ce_{Ce}^\times} = \mu^0_{Ce_{Ce}^\times} + k_B T \ln \frac{x_{Ce_{Ce}^\times}}{y_{Ce_{Ce}^\times}} , \tag{44}$$

$$\mu_{O_O^\times} = \mu^0_{O_O^\times} + k_B T \ln \frac{x_{O_O^\times}}{y_{O_O^\times}} , \tag{45}$$

where μ_i^0's ($i = Ce_{Ce}^\times$ or $O_O^\times$) are the virtual chemical potentials of host ions in their reference states. These are taken to be constants. Note that x_i's in Eqs. (44) and (45) are divided by their respective y_i's in order to conform to the definition of μ_α shown in Eq. (30). These expressions are also consistent with the definition of the Raoult's law, since $\mu_{Ce_{Ce}^\times} \to \mu^0_{Ce_{Ce}^\times}$ when $x_{Ce_{Ce}^\times} \to x^{max}_{Ce_{Ce}^\times} (=1 = y_{Ce_{Ce}^\times})$, and $\mu_{O_O^\times} \to \mu^0_{O_O^\times}$, when $x_{O_O^\times} \to x^{max}_{O_O^\times} (=2 = y_{O_O^\times})$. Here x_i^{max} is the maximum possible normalized concentrations of the i-type host ion in a perfect lattice.

Substituting the μ_α expression of Eq. (30) into Eqs. (40)–(43):

$$\ln\left[P_{O_2}^{1/2} \frac{x_{V_O^{\cdot\cdot}}}{\mathcal{F}_{V_O^{\cdot\cdot}}} \frac{x^2_{Ce'_{Ce}}}{\mathcal{F}^2_{Ce'_{Ce}}}\right] - \ln\frac{x_{O_O^\times}}{y_{O_O^\times}} - 2\ln\frac{x_{Ce_{Ce}^\times}}{y_{Ce_{Ce}^\times}} = -\frac{g_R}{k_B T} , \tag{46}$$

$$\ln\left[\frac{x_{V_O^{\cdot\cdot}}}{\mathcal{F}_{V_O^{\cdot\cdot}}} \frac{x_{Ce'_{Ce}}}{\mathcal{F}_{Ce'_{Ce}}} \frac{\mathcal{F}_{V_O^{\cdot}}}{x_{V_O^{\cdot}}}\right] - \ln\frac{x_{Ce_{Ce}^x}}{y_{Ce_{Ce}^\times}} = -\frac{g_2}{k_B T} , \tag{47}$$

$$\ln\left[\frac{x_{(CeV_O)^{\cdot}}}{\mathcal{F}_{(CeV_O)^{\cdot}}} \frac{\mathcal{F}_{V_O^{\cdot\cdot}}}{x_{V_O^{\cdot\cdot}}} \frac{\mathcal{F}_{Ce'_{Ce}}}{x_{Ce'_{Ce}}}\right] = -\frac{g_{B1}}{k_B T} , \tag{48}$$

$$\ln\left[\frac{x_{(CeV_O)^{\times}}}{\mathcal{F}_{(CeV_O)^{\times}}} \frac{\mathcal{F}_{V_O^{\cdot}}}{x_{V_O^{\cdot}}} \frac{\mathcal{F}_{Ce'_{Ce}}}{x_{Ce'_{Ce}}}\right] = -\frac{g_{B2}}{k_B T} . \tag{49}$$

Here g_R, g_2, g_{B1}, g_{B2} are the reaction free energies of the reactions shown in Eqs. (36)–(39), respectively, (note the correspondence with the g's defined at low defect concentration limit in Eqs. (64)–(67) of Sec. IV C). In particular g_{B1}, g_{B2} are the binding energies of the two different defect pairs. The ideal gas relationship, $\mu_{O_2} = k_B T \ln P_{O_2}$,[64] has been used in deriving Eq. (46). It is interesting to note that every x_α in the above equations is accompanied by its corresponding $\mathcal{F}_\alpha$ in the form of the $x_\alpha/\mathcal{F}_\alpha$ ratio.

The reaction free energies are given by

$$\begin{bmatrix} g_R \\ g_2 \\ g_{B1} \\ g_{B2} \end{bmatrix} = \begin{bmatrix} \mu^*_{V_O^{\cdot\cdot}} + 2\mu^*_{Ce'_{Ce}} - \mu^0_{O_O^\times} - 2\mu^0_{Ce_{Ce}^\times} \\ \mu^*_{V_O^{\cdot\cdot}} + \mu^*_{Ce'_{Ce}} - \mu^*_{V_O^{\cdot}} - \mu^0_{Ce_{Ce}^\times} \\ \mu^*_{(CeV_O)^{\cdot}} - \mu^*_{V_O^{\cdot\cdot}} - \mu_{Ce'_{Ce}} \\ \mu^*_{(CeV_O)^{\times}} - \mu^*_{V_O^{\cdot}} - \mu^*_{Ce'_{Ce}} \end{bmatrix} . \tag{50}$$

In addition, one has the charge neutrality condition

$$2x_{V_O^{\cdot\cdot}} + x_{V_O^{\cdot}} + x_{(CeV_O)^{\cdot}} = x_{Ce'_{Ce}} \tag{51}$$

and the structural conservation conditions

$$x^{max}_{Ce_{Ce}^\times} = x_{Ce_{Ce}^\times} + x_{Ce'_{Ce}} + x_{(CeV_O)^{\cdot}} + x_{(CeV_O)^{\times}} , \tag{52}$$

$$x^{max}_{O_O^\times} = x_{O_O^\times} + x_{V_O^{\cdot\cdot}} + x_{V_O^{\cdot}} + x_{(CeV_O)^{\cdot}} + x_{(CeV_O)^{\times}} . \tag{53}$$

The oxygen deficiency δ may then be obtained by summing up the concentrations of all oxygen vacancy containing defect species:

$$\delta = x_{V_O^{\cdot\cdot}} + x_{V_O^{\cdot}} + x_{(CeV_O)^{\cdot}} + x_{(CeV_O)^{\times}} . \tag{54}$$

B. Reaction free energies

The mean charges $\langle Q_c \rangle$ and $\langle Q_a \rangle$ may be obtained by averaging the charges of all building-block defects over their respective sublattices:

$$\begin{aligned}\langle Q_c \rangle &= (x_{\mathrm{Ce}'_{\mathrm{Ce}}} + x_{(\mathrm{Ce}V_{\mathrm{O}})^{\cdot}} + x_{(\mathrm{Ce}V_{\mathrm{O}})^{\times}}) Q_{\mathrm{Ce}'_{\mathrm{Ce}}} \\ &= -2\langle Q_a \rangle \\ &= -(x_{V_{\mathrm{O}}^{\cdot\cdot}} + x_{(\mathrm{Ce}V_{\mathrm{O}})^{\cdot}}) Q_{V_{\mathrm{O}}^{\cdot\cdot}} - (x_{V_{\mathrm{O}}^{\cdot}} + x_{(\mathrm{Ce}V_{\mathrm{O}})^{\times}}) Q_{V_{\mathrm{O}}^{\cdot}} ,\end{aligned} \tag{55}$$

where $Q_{\mathrm{Ce}'_{\mathrm{Ce}}}(=-|e|)$, $Q_{V_{\mathrm{O}}^{\cdot\cdot}}(=+2|e|)$, and $Q_{V_{\mathrm{O}}^{\cdot}}(=+|e|)$ are the charges of the building-block defects, respectively, $\mathrm{Ce}'_{\mathrm{Ce}}$, $V_{\mathrm{O}}^{\cdot\cdot}$, and $V_{\mathrm{O}}^{\cdot}$. Here the relationship between $\langle Q_c \rangle$ and $\langle Q_a \rangle$ in Eq. (9) has been used. Differentiating Eq. (55) with respect to the defect concentrations, one has

$$\begin{aligned}&\frac{\partial\langle Q_c \rangle}{\partial x_{\mathrm{Ce}'_{\mathrm{Ce}}}} = \frac{\partial\langle Q_c \rangle}{\partial x_{V_{\mathrm{O}}^{\cdot}}} = \frac{\partial\langle Q_c \rangle}{\partial x_{(\mathrm{Ce}V_{\mathrm{O}})^{\cdot}}} = \frac{\partial\langle Q_c \rangle}{\partial x_{(\mathrm{Ce}V_{\mathrm{O}})^{\times}}} = -|e| , \\ &\frac{\partial\langle Q_c \rangle}{\partial x_{V_{\mathrm{O}}^{\cdot\cdot}}} = -2|e| ,\end{aligned} \tag{56}$$

Combining Eqs. (27), (50), (55), and (56) the reaction free energies may be written as functions of the defect concentrations. This is shown below in matrix form:

$$\begin{bmatrix} g_R \\ g_2 \\ g_{B1} \\ g_{B2} \end{bmatrix} = \begin{bmatrix} g_R^* \\ g_2^* \\ g_{B1}^* \\ g_{B2}^* \end{bmatrix} - \frac{|e|}{4\pi\varepsilon_r\varepsilon_0}(\mathcal{L}) \begin{bmatrix} x_{\mathrm{Ce}'_{\mathrm{Ce}}} \\ x_{V_{\mathrm{O}}^{\cdot\cdot}} \\ x_{V_{\mathrm{O}}^{\cdot}} \\ x_{(\mathrm{Ce}V_{\mathrm{O}})^{\cdot}} \\ x_{(\mathrm{Ce}V_{\mathrm{O}})^{\times}} \end{bmatrix} , \tag{57}$$

where the g^*'s are the concentration independent components

$$\begin{bmatrix} g_R^* \\ g_2^* \\ g_{B1}^* \\ g_{B2}^* \end{bmatrix} = \begin{bmatrix} g^{\mathrm{I}}_{V_{\mathrm{O}}^{\cdot\cdot}} + 2g^{\mathrm{I}}_{\mathrm{Ce}'_{\mathrm{Ce}}} - \mu^{\mathrm{O}}_{\mathrm{O}^{\times}_{\mathrm{O}}} - 2\mu^{\mathrm{O}}_{\mathrm{Ce}^{\times}_{\mathrm{Ce}}} \\ g^{\mathrm{I}}_{V_{\mathrm{O}}^{\cdot\cdot}} + g^{\mathrm{I}}_{\mathrm{Ce}'_{\mathrm{Ce}}} - g^{\mathrm{I}}_{V_{\mathrm{O}}^{\cdot}} - \mu^{0}_{\mathrm{Ce}^{\times}_{\mathrm{Ce}}} \\ g^{\mathrm{I}}_{(\mathrm{Ce}V_{\mathrm{O}})^{\cdot}} - g^{\mathrm{I}}_{V_{\mathrm{O}}^{\cdot\cdot}} - g^{\mathrm{I}}_{\mathrm{Ce}'_{\mathrm{Ce}}} \\ g^{\mathrm{I}}_{(\mathrm{Ce}V_{\mathrm{O}})^{\times}} - g^{\mathrm{I}}_{V_{\mathrm{O}}^{\cdot}} - g^{\mathrm{I}}_{\mathrm{Ce}'_{\mathrm{Ce}}} \end{bmatrix} \tag{58}$$

and the $(\mathcal{L})$ matrix is

$$(\mathcal{L}) = \begin{bmatrix} 6\mathcal{L}_{\mathrm{Ce}'_{\mathrm{Ce}}} + \mathcal{L}_{V_{\mathrm{O}}^{\cdot}} & 4\mathcal{L}_{V_{\mathrm{O}}^{\cdot\cdot}} & 4\mathcal{L}_{V_{\mathrm{O}}^{\cdot}} & 2\mathcal{L}_{\mathrm{Ce}'_{\mathrm{Ce}}} + \mathcal{L}_{V_{\mathrm{O}}^{\cdot\cdot}} + 4\mathcal{L}_{(\mathrm{Ce}V_{\mathrm{O}})^{\cdot}} & 2\mathcal{L}_{\mathrm{Ce}'_{\mathrm{Ce}}} + \mathcal{L}_{V_{\mathrm{O}}^{\cdot\cdot}} + 4\mathcal{L}_{(\mathrm{Ce}V_{\mathrm{O}})^{\times}} \\ 3\mathcal{L}_{\mathrm{Ce}'_{\mathrm{Ce}}} + \mathcal{L}_{V_{\mathrm{O}}^{\cdot\cdot}} - \mathcal{L}_{V_{\mathrm{O}}^{\cdot}} & 2\mathcal{L}_{V_{\mathrm{O}}^{\cdot\cdot}} & 2\mathcal{L}_{V_{\mathrm{O}}^{\cdot}} & \mathcal{L}_{\mathrm{Ce}'_{\mathrm{Ce}}} + \mathcal{L}_{V_{\mathrm{O}}^{\cdot\cdot}} - \mathcal{L}_{V_{\mathrm{O}}^{\cdot}} + 2\mathcal{L}_{(\mathrm{Ce}V_{\mathrm{O}})^{\cdot}} & \mathcal{L}_{\mathrm{Ce}'_{\mathrm{Ce}}} + \mathcal{L}_{V_{\mathrm{O}}^{\cdot\cdot}} - \mathcal{L}_{V_{\mathrm{O}}^{\cdot}} + 2\mathcal{L}_{(\mathrm{Ce}V_{\mathrm{O}})^{\times}} \\ -3\mathcal{L}_{\mathrm{Ce}'_{\mathrm{Ce}}} - \mathcal{L}_{V_{\mathrm{O}}^{\cdot\cdot}} + \mathcal{L}_{(\mathrm{Ce}V_{\mathrm{O}})^{\cdot}} & -2\mathcal{L}_{V_{\mathrm{O}}^{\cdot\cdot}} & -2\mathcal{L}_{V_{\mathrm{O}}^{\cdot}} & -\mathcal{L}_{\mathrm{Ce}'_{\mathrm{Ce}}} - \mathcal{L}_{V_{\mathrm{O}}^{\cdot\cdot}} - 4\mathcal{L}_{(\mathrm{Ce}V_{\mathrm{O}})^{\cdot}} & -\mathcal{L}_{\mathrm{Ce}'_{\mathrm{Ce}}} - \mathcal{L}_{V_{\mathrm{O}}^{\cdot\cdot}} + \mathcal{L}_{(\mathrm{Ce}V_{\mathrm{O}})^{\cdot}} - 2\mathcal{L}_{(\mathrm{Ce}V_{\mathrm{O}})^{\times}} \\ -2\mathcal{L}_{\mathrm{Ce}'_{\mathrm{Ce}}} - \mathcal{L}_{V_{\mathrm{O}}^{\cdot}} + \mathcal{L}_{(\mathrm{Ce}V_{\mathrm{O}})^{\times}} & -\mathcal{L}_{V_{\mathrm{O}}^{\cdot\cdot}} & -\mathcal{L}_{V_{\mathrm{O}}^{\cdot}} & -\mathcal{L}_{\mathrm{Ce}'_{\mathrm{Ce}}} - \mathcal{L}_{V'_{\mathrm{O}}} - \mathcal{L}_{(\mathrm{Ce}V_{\mathrm{O}})^{\cdot}} + \mathcal{L}_{(\mathrm{Ce}V_{\mathrm{O}})^{\times}} & -\mathcal{L}_{\mathrm{Ce}'_{\mathrm{Ce}}} - \mathcal{L}_{V_{\mathrm{O}}^{\cdot}} \end{bmatrix} \tag{59}$$

The free energies can be further separated into their enthalpy and entropy components:

$$\begin{bmatrix} g_R^* \\ g_2^* \\ g_{B1}^* \\ g_{B2}^* \end{bmatrix} = \begin{bmatrix} h_R^* \\ h_2^* \\ h_{B1}^* \\ h_{B2}^* \end{bmatrix} - T \begin{bmatrix} s_R^* \\ s_2^* \\ s_{B1}^* \\ s_{B2}^* \end{bmatrix} , \tag{60}$$

where h^*'s and s^*'s are independent of the defect concentrations. Substitute Eq. (60) back into Eq. (57):

$$\begin{bmatrix} g_R \\ g_2 \\ g_{B1} \\ g_{B2} \end{bmatrix} = \begin{bmatrix} h_R \\ h_2 \\ h_{B1} \\ h_{B2} \end{bmatrix} - T \begin{bmatrix} s_R^* \\ s_2^* \\ s_{B1}^* \\ s_{B2}^* \end{bmatrix} , \tag{61}$$

where the reaction enthalpies are found to be functions of defect concentrations and are given by

$$\begin{bmatrix} h_R \\ h_2 \\ h_{B1} \\ h_{B2} \end{bmatrix} = \begin{bmatrix} h_R^* \\ h_2^* \\ h_{B1}^* \\ h_{B2}^* \end{bmatrix} - \frac{|e|}{4\pi\varepsilon_r\varepsilon_0}(\mathcal{L}) \begin{bmatrix} x_{\mathrm{Ce}'_{\mathrm{Ce}}} \\ x_{V_{\mathrm{O}}^{\cdot\cdot}} \\ x_{V_{\mathrm{O}}^{\cdot}} \\ x_{(\mathrm{Ce}V_{\mathrm{O}})^{\cdot}} \\ x_{(\mathrm{Ce}V_{\mathrm{O}})^{\times}} \end{bmatrix} . \tag{62}$$

Notice that in the above derivations the defect concentration dependence of the entropy terms is assumed to be negligible.

C. Correspondence to traditional defect theory

A good test for the validity of the current formulation is to see if Eqs. (46)–(49) are equivalent to the well established traditional mass action equations in the limit of low defect concentrations. By setting $x_\alpha \to 0$, it is found that $\langle Q_c \rangle \cong 0$ from Eq. (55), $\mu_\alpha^* \cong g_\alpha^{\mathrm{I}}$ from Eq. (27), and $\ln \mathcal{F}_\alpha \cong \ln y_\alpha$ from Eq. (29). Under these conditions the ex-

pression for the virtual chemical potential in Eq. (30) is simplified to

$$\mu_\alpha \cong g_\alpha^{\mathrm{I}} + k_B T \ln\left[\frac{x_\alpha}{y_\alpha}\right], \tag{63}$$

which is the Henry's law.[7,64] From Eq. (57) one also obtains $g_R \cong g_R^*$, $g_2 \cong g_2^*$, $g_{B1} \cong g_{B1}^*$, $g_{B2} \cong g_{B2}^*$, and from Eqs. (52) and (53) one has $x_{\mathrm{Ce}_{\mathrm{Ce}}^\times} \cong x_{\mathrm{Ce}_{\mathrm{Ce}}^\times}^{\max}$ $(=1=y_{\mathrm{Ce}_{\mathrm{Ce}}^\times})$ and $x_{\mathrm{O}_{\mathrm{O}}^\times} \cong x_{\mathrm{O}_{\mathrm{Ce}}^\times}^{\max}$ $(=2=y_{\mathrm{O}_{\mathrm{O}}^\times})$, respectively. Using the y values listed in Table I, it is easy to show that Eqs. (46)–(49) are now simplified to

$$\ln(P_{\mathrm{O}_2}^{1/2} x_{V_{\mathrm{O}}^{\cdot\cdot}} x_{\mathrm{Ce}_{\mathrm{Ce}}'}^2) = -\frac{g_R^*}{k_B T} + \ln 2 , \tag{64}$$

$$\ln\left[\frac{x_{V_{\mathrm{O}}^{\cdot\cdot}} x_{\mathrm{Ce}_{\mathrm{Ce}}'}}{x_{V_{\mathrm{O}}^{\cdot}}}\right] = -\frac{g_2^*}{k_B T} , \tag{65}$$

$$\ln\left[\frac{x_{(\mathrm{Ce}V_{\mathrm{O}})^{\cdot}}}{x_{V_{\mathrm{O}}^{\cdot\cdot}} x_{\mathrm{Ce}_{\mathrm{Ce}}'}}\right] = -\frac{g_{B1}^*}{k_B T} + \ln\frac{Z_c}{2} , \tag{66}$$

$$\ln\left[\frac{x_{(\mathrm{Ce}V_{\mathrm{O}})^{\times}}}{x_{V_{\mathrm{O}}^{\cdot}} x_{\mathrm{Ce}_{\mathrm{Ce}}'}}\right] = -\frac{g_{B2}^*}{k_B T} + \ln\frac{Z_c}{2} , \tag{67}$$

which are the traditional mass action equations.[4,5,36] Notice that the defect concentrations here may also be written in the form of the x_α / y_α ratio, which parallels the $x_\alpha / \mathcal{F}_\alpha$ form of the general formulation shown in Eqs. (46)–(49).

V. RESULTS AND DISCUSSIONS

This section presents the results obtained from the application of the general defect chemistry formulations developed in the previous sections to the oxygen deficient $\mathrm{CeO}_{2-\delta}$ system. The defect concentrations are calculated by solving the set of simultaneous equations (46)–(53) using the numerical algorithm described in the Appendix.

A. Parameters required for calculations

The parameters required for the calculations are listed in Table I, which includes the values of $\Lambda_{\alpha,\beta}$, y_α, $x_\alpha^{\max}$, as well as the expressions for $\mathcal{L}_\alpha$. The expressions for the reaction free energies, g's, are provided in Eq. (57). Also, $\varepsilon_r = 25$ for CeO_2,[66] $Z_c = 8$, $Z_a = 4$, and the nearest neighbor $\mathrm{O}_{\mathrm{O}}^\times$ to $\mathrm{Ce}_{\mathrm{Ce}}^\times$ distance is $l_0 = 2.706$ Å.[41] In addition the h^*'s and s^*'s (in the form of preexponentials) shown in Eqs. (60) and (61) are needed as input parameters to the calculations.

The $\mathcal{L}_\alpha$ expressions listed in Table I require M_c and M_a. These Madelung constants may be obtained from their definitions in Eqs. (11) and (12) by carrying out the summations over a spherical volume centered at the reference site, and increase the sphere radius r until convergence occurs.[46] The results of these calculations are shown in Fig. 3. It can be seen that the summations converge at $r > 100$ (in unit of l_0), and give $M_c = -2.62 \times 10^{-9}$ C/m, and $M_a = 4.27 \times 10^{-9}$ C/m.

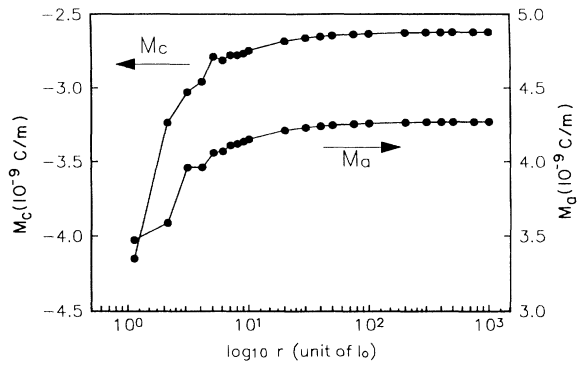

FIG. 3. Plots of M_c and M_a vs the summation radius r, where r is in unit of $l_0 = 2.706$ Å.

To simplify the calculations, the $\mathcal{L}_\alpha$ expressions are obtained from Eq. (14) using the smallest possible short-range interaction envelopes that enclose only the building-block defects (for example, see the solid line envelope in Fig. 1). The exclusion factors $\Lambda_{\alpha,\beta}$ are similarly obtained using the smallest possible exclusion zones enclosing the lattice sites occupied by the building-block defects (see Fig. 2). In actuality the sizes of these envelopes are functions of the short-range interactions, and are expected to be larger than those used here. Nevertheless, a number of calculations carried out using zones of different sizes have shown that, while the defect concentrations obtained are modified slightly, the general conclusions presented in this paper are still valid.

B. Oxygen deficiency and defect concentrations

Using trial values of h^* and s^* as input parameters, the defect concentrations are calculated and the oxygen deficiency δ has been obtained using Eq. (54). The values of these input parameters are adjusted until a best fit (by eyes) is obtained between the calculated and the experimental δ values. These best fit h^* and s^* values are listed in Table II. The calculated best fit δ values are shown in

TABLE II. Comparison of the enthalpy and enthropy parameters used in the present study and that reported in the literature.

	This calculation	Literature
h_R^* (eV)	5.00	4.67[a]
h_2^* (eV)	0.17	0.56[a]
h_{B1}^* (eV)	−0.25	−0.25[b]
h_{B2}^* (eV)	−0.15	
$\exp(s_R^*/k_B)$ (atm$^{1/2}$)	1.47×10^7	3.73×10^6[a]
$\exp(s_2^*/k_B)$	2.83×10^{-2}	2.38[a]
$\exp(s_{B1}^*/k_B)$	1.0	
$\exp(s_{B2}^*/k_B)$	2.21	

[a]Reference 36.
[b]Reference 59.

Figs. 4 and 5, which are plotted vs P_{O_2} at fixed temperatures. The experimental δ values shown in these diagrams have been compiled by Tuller *et al.* [35] These data were originally measured by Bevan and Kordis,[31] and Panlener, Blumenthal, and Garnier,[67] Iwasaki and Katsura,[68] and Sørensen.[69] From Fig. 4 it can be seen that the agreement is good in general, except in two regions where the calculated δ values are larger than that of the experimental observations: at $T \geq 1300\,°C$ and $\delta > 10^{-1}$; at $T \leq 900\,°C$ and $\delta > 10^{-2}$. Possible causes of these disagreements will be discussed later in this section.

Plotted in Fig. 5 as a typical example are the calculated concentrations of different defect species. This plot may be roughly divided into three P_{O_2} regimes, each of which has the oxygen deficiency dominated by a different point-defect species and hence, according to the traditional theory, is expected to have a characteristic gradient to the δ curve.[35,36] These gradients are also shown in the diagram as the hypothenuses of the triangles. The dominating species at high P_{O_2} ($\log_{10}P_{O_2} > -5$) is $V_O^{\cdot\cdot}$ which gives a gradient of $-\frac{1}{6}$. At intermediate P_{O_2} ($-5 > \log_{10}P_{O_2} > -10$) $V_O^{\cdot}$ dominates and gives a gradient of $-\frac{1}{4}$. At low P_{O_2}($\log_{10}P_{O_2} < -10$), assuming $(CeV_O)^{\times}$ dominance, the expected gradient is $-\frac{1}{2}$. As can be seen in Fig. 5 the gradients of the δ curve in the high and intermediate P_{O_2} regimes agree well with the predictions of the traditional theory. At low P_{O_2}, however, the δ curve bends over such that its gradient becomes much shallower than the predicted value of $-\frac{1}{2}$. This deviation from the traditional theory is clearly caused by the strong interaction and exclusion effects that arise at high defect concentrations (here $\delta > 10^{-1}$).

It is noted in Fig. 4 that the experimentally observed δ value rises sharply at $T \leq 900\,°C$ in the low P_{O_2} range when $\delta > 10^{-2}$. In fact at $T = 800\,°C$ and $\log_{10}P_{O_2} \sim -20$ the δ curve has a gradient close to $-\frac{1}{2}$. According to the traditional defect theory there are two defect species that,

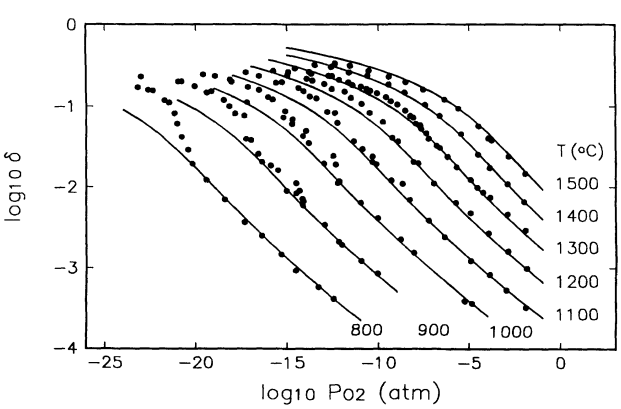

FIG. 4. Plot of $\log_{10}\delta$ vs $\log_{10}P_{O_2}$ at different temperatures. δ is the oxygen deficiency in $CeO_{2-\delta}$. Solid curves are from calculations. Filled circles are experimental data compiled by Tuller and Nowick, Ref. 35.

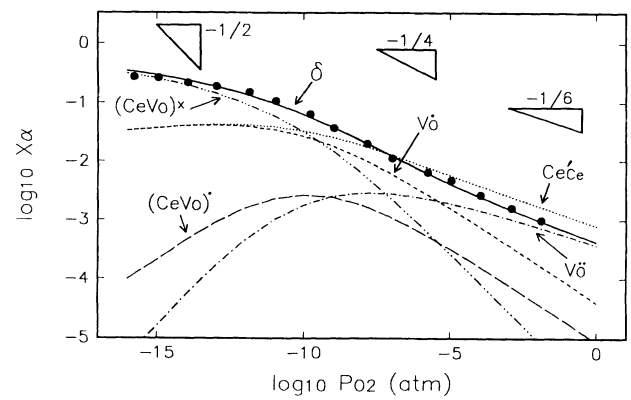

FIG. 5. Plot of calculated $\log_{10}x_\alpha$ vs $\log_{10}P_{O_2}$ at $T = 1200\,°C$. Solid curve is the calculated δ, and filled circles are the experimental data compiled by Tuller and Nowick (Ref. 35). The hypotenuse of the triangles have gradients indicated by the accompanying numbers.

when dominating, may give rise to this kind of behavior. The first species is $(CeV_O)^{\times}$, which is the one that is being utilized in the current calculations. The second species is $V_O^{\times}$, which may be formed according to the reaction:

$$V_O^{\cdot} + Ce'_{Ce} \leftrightarrow V_O^{\times} + Ce_{Ce}^{\times} \,. \tag{68}$$

Based on this alternative $V_O^{\times}$ assumption, additional calculations had been conducted. The resulting δ curves (not shown here) exhibit steep gradients close to $-\frac{1}{2}$ in the low P_{O_2} regimes. These curves, however, do not bend over until a fairly high δ value of ~ 1.5, which, in principle, is an acceptable value in view of the fact that it is still less than $x_{V_O^{\times}}^{\max} = 2$. This value, however, is clearly much higher than the experimentally measured δ shown in Fig. 4, which has, for example, maximum $\delta \sim 0.3$ at $T = 1500\,°C$. As a result of this disagreement, the $V_O^{\times}$ alternative has been ruled out. It can thus be concluded that the oxygen deficiency in the low P_{O_2} regime is dominated by the $(CeV_O)^{\times}$ species. The observed discrepancy in the low-T and low-P_{O_2} regime may then be explained by the appearance of new crystalline phase not accounted for in the current calculations, such as the low-temperature CeO_2 phase reported by Bevan and Kordis.[31]

Figure 4 also shows that, at $T \geq 1300\,°C$ in the low P_{O_2} regime when $\delta > 10^{-1}$, the calculated oxygen deficiency is slightly larger than the observed values. This may be caused by the fact that the calculations have used the smallest possible interaction and exclusion envelopes as mentioned in Sec. V A, such that the values of both $\mathcal{L}_\alpha$ and $\Lambda_{\alpha,\beta}$ are smaller than their actual values. It is expected that with larger envelopes the values of $\mathcal{L}_\alpha$ and $\Lambda_{\alpha,\beta}$ would become greater, which in turn may lead to a better fit of the calculations to the experimental data. This is because greater $\mathcal{L}_\alpha$ values mean stronger defect interactions that would bend the δ curve over sooner, and

greater $\Lambda_{\alpha,\beta}$ values mean larger reduction in the available lattice space that would lower the maximum attainable δ value.

Table II also lists the h^* and s^* values reported in the literature for comparison purpose. It is noted that due to the low $x_{(CeV_O)^{\cdot}}$ concentration (see Fig. 5) h^*_{B1} and s^*_{B1} were not able to be fitted. As a result their literature values have been used directly in the calculations without adjustment. From Table II it is clear that the agreement between the values obtained in the present work and the literature values is acceptable except in the cases of h^*_2 and s^*_2. This may be explained by noticing that these literature values were obtained by applying the traditional theory to the experimental data measured in intermediate P_{O_2} regime, which was assumed to be dominated by $V_O^{\cdot}$.[35,36] From Fig. 5 it can be seen that in this P_{O_2} range $\delta > x_{V_O^{\cdot}}$ and that the oxygen deficiency has significant contributions from other species, including $V_O^{\cdot\cdot}$ and $(CeV_O)^{\times}$. Furthermore the δ value here is greater than 10^{-2}, indicating high defect concentrations that can lead to behavior deviating from the prediction of traditional theory. Together these factors may have led to an inaccurate result acquired from analyses based on the traditional theory using the assumption of the complete dominance by the $V_O^{\cdot}$ species.

C. Effects of defect interactions and exclusions

The μ_α expression given in Eq. (30), as pointed out in Sec. III, allows one to turn the effects of defect interaction and exclusion on and off individually. Figure 6 shows the results obtained for $T=1200°C$ using (*A*) both effects, (*B*) exclusion effect only, (*C*) interaction effect only, and (*D*) neither effect. Note that case (*D*) corresponds to the traditional theory. For purpose of clarity only the curves calculated for $(CeV_O)^{\times}$ are shown in Fig. 6, but the same observations described here are applicable to all the other species.

Comparing curves (*A*) and (*D*), it can be seen that they coincide at high P_{O_2} where the defect concentrations are low. Curve (*A*), however, begins to bend over and deviate from curve (*D*) as P_{O_2} is reduced to $\log_{10}P_{O_2} < -6$, which, according to Fig. 5, occurs when δ begins to exceed 8×10^{-3}. It is interesting to note that this δ value, which indicates the level where the traditional theory begins to break down, is consistent with Wagner's observation in CoO in which the defect concentrations were found to deviate from the traditional ideal behavior at a level of 6×10^{-3}.[13] The same kind of deviation behavior is also observed in curves (*B*) and (*C*).

Curve (*D*) in Fig. 6 displays some behavior that is physically impossible. It rises monotonically with decreasing P_{O_2}, and has $\log_{10}x_{(CeV_O)^{\times}} > 0$ (i.e., $x_{(CeV_O)^{\times}} > x^{max}_{(CeV_O)^{\times}} = 1$) at $\log_{10}P_{O_2} < -14$. This clearly demonstrates the well known inadequacy of the traditional theory at high defect concentrations. Curves (*A*), (*B*), and (*C*), on the other hand, all bend over with decreasing P_{O_2} and do not exceed the limit of $\log_{10}x^{max}_{(CeV_O)^{\times}} = 0$. This observation clearly shows that in the calculations the interaction and exclusion effects can limit the defect concentrations down to more realistic values. The fact that curve (*C*) bends more than (*B*) indicates that interaction is more effective in this regard than exclusion. It is nevertheless worthwhile to remember that in nonionic systems (for example, covalent crystals) in which the point defects may be uncharged and that the Coulombic interaction may become negligible, such that the high-concentration defect chemistry can be dominated by the exclusion effect.

The interaction effect influences the defect concentrations by modifying reaction enthalpies through Eq. (62). Using this equation the h values are calculated and plotted in Fig. 7 as functions of P_{O_2} at $T=1200°C$. Here the h values approach that of h^* when defect concentrations are low at high P_{O_2}. As defect concentrations increase with reducing P_{O_2}, however, the h values begin to change. The h_R, h_2 values become larger which, from Eqs. (46) and (47), suggest that it is more difficult to form $V_O^{\cdot\cdot}$ and $V_O^{\cdot}$, respectively. The h_{B1}, h_{B2} values become more negative which, from Eqs. (48) and (49), suggest that it is easier to form $(CeV_O)^{\cdot}$ and $(CeV_O)^{\times}$, respective-

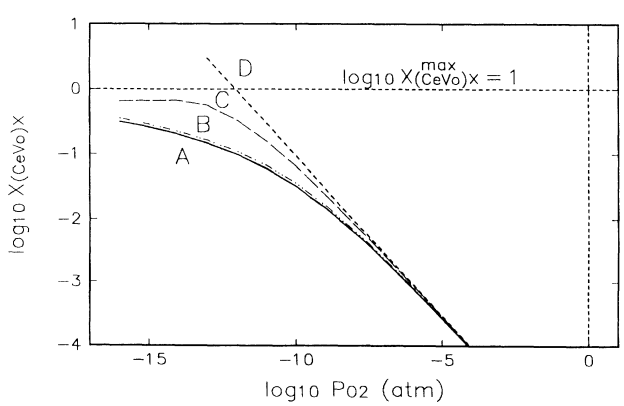

FIG. 6. Plot of calculated $\log_{10}x_{(CeV_O)^{\times}}$ vs $\log_{10}P_{O_2}$. Calculations include the effects of (*A*) both interactions and exclusions, (*B*) exclusions only, (*C*) interactions only, and (*D*) neither interactions nor exclusions (traditional theory). $T=1200°C$.

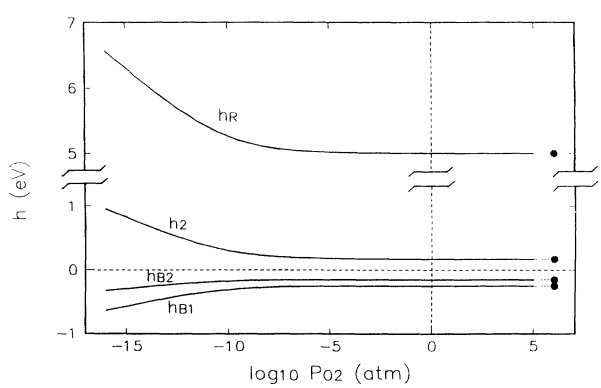

FIG. 7. Plot of calculated reaction enthalpies h vs $\log_{10}P_{O_2}$. $T=1200°C$. The filled circles are the low-defect-concentration limiting values h^*.

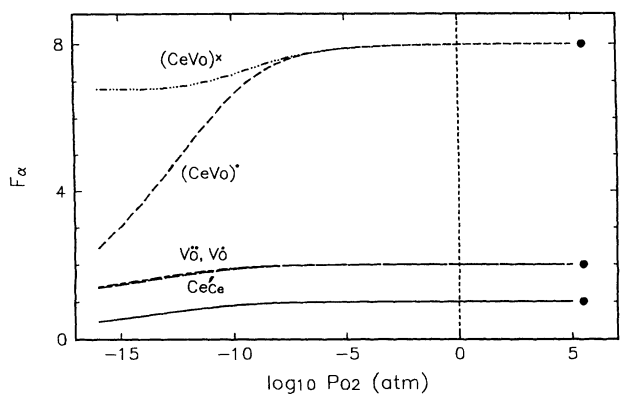

FIG. 8. Plot of calculated exclusion functions $\mathcal{F}_\alpha$ vs $\log_{10}P_{O_2}$. $T=1200\,°C$. The filled circles are the low-defect-concentration limiting values, y_α.

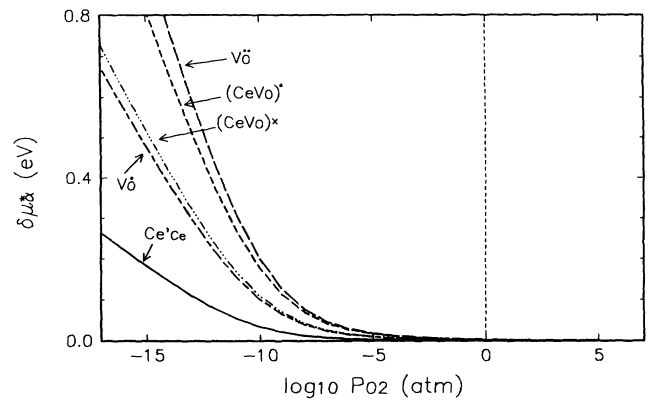

FIG. 9. Plots of $\delta\mu_\alpha^*$ vs $\log_{10}P_{O_2}$ at $T=1200\,°C$.

ly. It is noted that the net change in the enthalpies $(h-h^*)$ at $\log_{10}P_{O_2}=-15$ is about 1.6 eV in the case of h_R, and -0.45 eV in the case of h_{B1}. These values are much larger than that calculated for the Debye-Hückel-type corrections, which is typically of the order of 0.1 eV.[10,70] This indicates that Debye-Hückel-type correction is inadequate at high defect concentrations.

The exclusion effect influences the defect concentrations by modifying exclusion functions $\mathcal{F}_\alpha$ through Eq. (29). Using this equation the $\mathcal{F}_\alpha$ values are calculated and plotted in Fig. 8 as functions of P_{O_2} at $T=1200\,°C$. Here the $\mathcal{F}_\alpha$ values approach that of y_α when defect concentrations are low at high P_{O_2}. As defect concentrations increase with reducing P_{O_2}, however, the $\mathcal{F}_\alpha$ values begin to drop. This drop is much more severe in the case of $(CeV_O)^{\cdot}$ than that of the other species. The $(CeV_O)^{\times}$ is the only case in which the drop of the curve plateaus out at $\mathcal{F}_{(CeV_O)^{\times}}\sim 6.8$ around $\log_{10}P_{O_2}\sim -15$. This is consistent with the fact that at low P_{O_2} the lattice is dominated by $(CeV_O)^{\times}$, as can be seen from Fig. 5. This also indicates that a large fraction of the lattice is now devoid of other defect species, and hence is available for the placement of the $(CeV_O)^{\times}$ pair.

D. Thermodynamic activity of point defect

Using Eq. (34) the changes in the virtual chemical potentials $\delta\mu_\alpha^*$ are calculated at $T=1200\,°C$, and the results are plotted against $\log_{10}P_{O_2}$ in Fig. 9. Here it is found for all defect species that $\delta\mu_\alpha^*\to 0$ as $\log_{10}P_{O_2}\to 0$, and that $\delta\mu_\alpha^*$ increases with decreasing $\log_{10}P_{O_2}$. This observation demonstrates the positive correlation between $\delta\mu_\alpha^*$ and the defect concentrations. From this figure it can also be seen that, at constant P_{O_2}, the $\delta\mu_\alpha^*$ values appear to have the following relationship:

$$\delta\mu^*_{V_O^{\cdot\cdot}}\approx\delta\mu^*_{(CeV_O)^{\cdot}}>\delta\mu^*_{(CeV_O)^{\times}}\approx\delta\mu^*_{V_O^{\cdot}}>\delta\mu^*_{Ce'_{Ce}}\ . \quad (69)$$

Noticing that $(CeV_O)^{\cdot}$ contains a $V_O^{\cdot\cdot}$, and $(CeV_O)^{\times}$ contains a $V_O^{\cdot}$, this observation suggests that the magnitude of the change in μ_α^* is strongly correlated to the type of anionic component of the particular defect species. In other words, those defects that contain $V_O^{\cdot\cdot}$ component have the largest $\delta\mu_\alpha^*$ value, which are followed by those that contain $V_O^{\cdot}$, which in turn are followed by Ce'_{Ce} that does not have any anionic component.

From Eq. (35) it can be seen that the defect thermodynamic activity a_α is a function of the defect concentrations x_α. Using this equation the defect activities are calculated at $T=1200\,°C$, and the results are plotted as functions of $\log_{10}P_{O_2}$ in Fig. 10. At low defect concentrations, the behavior of these curves is similar to that of their x_α counterparts in Fig. 5. An examination of the regimes of $\log_{10}P_{O_2}>-5$ in these two diagrams shows that the curves that correspond to the same species are parallel to each other. This is not surprising because here at low defect concentrations $\mathcal{F}_\alpha\cong y_\alpha$, $\delta\mu_\alpha^*\cong 0$ eV such that $a_\alpha\propto x_\alpha$. This observation is consistent with Henry's law.[64] In the regime of high defect concentration $(\log_{10}P_{O_2}<-10)$ $\mathcal{F}_\alpha$ deviates from y_α, $\delta\mu_\alpha^*$ deviates from 0 eV, and as a result the curves in Figs. 5 and 10 are no longer parallel.

The proportionality between a_α and x_α in the low-

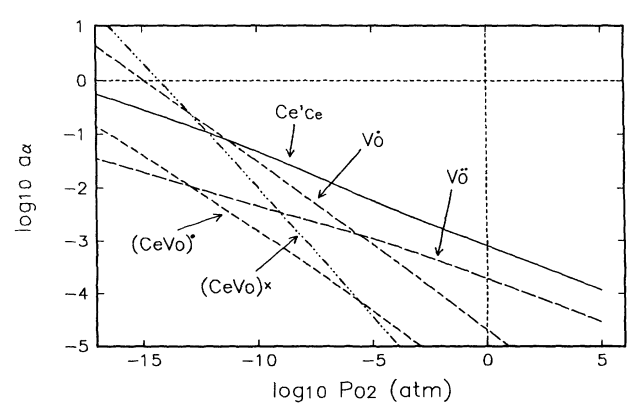

FIG. 10. Plots of $\log_{10}a_\alpha$ vs $\log_{10}P_{O_2}$ at $T=1200\,°C$.

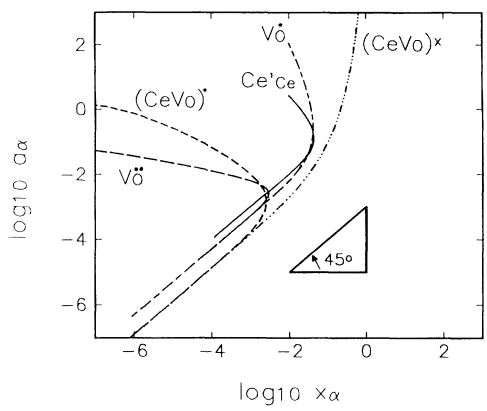

FIG. 11. Plots of $\log_{10}a_\alpha$ vs $\log_{10}x_\alpha$ at $T=1200\,^\circ\mathrm{C}$. The hypotenuse of the triangle is at 45° to the $\log_{10}x_\alpha$ axis.

defect-concentration regime can again be observed in Fig. 11, which plots $\log_{10}a_\alpha$ vs $\log_{10}x_\alpha$ at $T=1200\,^\circ\mathrm{C}$. Here it is observed that when the values of x_α are low, all the curves are straight lines that make an angle of 45° to the $\log_{10}x_\alpha$ axis. This clearly indicates the $a_\alpha \propto x_\alpha$ relationships. The curves of similar species tend to bunch together: those of the two vacancy species form one group, those of the pair species form another group, and that of $\mathrm{Ce}'_{\mathrm{Ce}}$ forms a third group. It is also seen that all curves turn around at large x_α values, indicating that a_α is not a single valued function of x_α. This observation does not agree with the traditional thermodynamic definition of a_α, which requires the activity to be a monotonic function of the concentration.[64] The disagreement may arise because the system being studied here involves defects that are strongly interacting, which is a factor that is typically not considered in the traditional thermodynamic formulation.

VI. CONCLUSIONS

This work describes a statistical thermodynamic formulation of crystalline point-defect chemistry that has general applicability at all levels of defect concentrations. The focus of this approach is an expression for the virtual chemical potential of defect μ_α, which is derived from the system Gibbs free energy that explicitly incorporates the contributions from defect interaction, and that from a configurational entropy that incorporates the generalized defect exclusion. Using this μ_α expression in a manner similar to that of the traditional theory, a set of equations is established and solved to obtain defect concentrations as explicit functions of environmental parameters.

The applicability of the formulation developed is demonstrated first by showing its equivalence with traditional defect chemistry formulation at low concentration limit, and then by working out a detailed example using the undoped nonstoichiometric $\mathrm{CeO}_{2-\delta}$ as a model system. In this example, the calculated oxygen deficiency is found to be in good agreement with literature data. This study also shows that the dominating species in the low-P_{O_2} regime is $(\mathrm{Ce}V_{\mathrm{O}})^\times$, rather than $V_{\mathrm{O}}^\times$. The interaction and exclusion effects are found to influence the defect chemistry by modifying, respectively, the reaction enthalpies h's and the exclusion function $\mathcal{F}_\alpha$'s. The net result of these two effects is the lowering of the calculated defect concentrations to values that are realistic compared to that obtained using the traditional theory. Examinations of the defect activities show some nontraditional behavior, which apparently is related to the strong interacting nature of the defect system, which is a factor usually not included in the traditional thermodynamic considerations.

ACKNOWLEDGMENTS

The author would like to thank Dr. T. A. Ramanarayanan and Dr. V. Pareek for their useful discussions that motivated this work.

APPENDIX: ALGORITHM FOR DEFECT CONCENTRATION CALCULATIONS

A reliable general methodology for calculating point defect concentrations can be very useful. Accordingly the authors report here a numerical algorithm that has been developed to calculate x_α values as functions of P_{O_2} at a fixed T.

Calculation of the equilibrium defect concentrations is not a trivial task. Even in the limit of low defect concentrations, which allows simpler mathematics, it still involves solving simultaneously the mass action equations of Eqs. (64)–(67), and the constant equations of Eqs. (51)–(53). Previously this was accomplished with some effort by combining all the equations to give a polynomial in terms of x_α's, which is then solved.[10,71,72] This approach, however, is not applicable in the more general situation where it is necessary to solve a set of simultaneous equations, including Eqs. (46)–(53), that contain complex and convoluted functions of x_α's, such as $\mathcal{F}_\alpha$ [see Eq. (29)] and the reaction enthalpies [see Eq. (57)].

Let us rewrite Eqs. (46)–(49) and (51)–(53) into the following forms:

$$\chi_a=\ln\left[P_{\mathrm{O}_2}^{1/2}\frac{x_{V_{\mathrm{O}}^{\cdot\cdot}}}{\mathcal{F}_{V_{\mathrm{O}}^{\cdot\cdot}}}\frac{x^2_{\mathrm{Ce}'_{\mathrm{Ce}}}}{\mathcal{F}^2_{\mathrm{Ce}'_{\mathrm{Ce}}}}\right]-\ln\frac{x_{\mathrm{O}_{\mathrm{O}}^\times}}{y_{\mathrm{O}_{\mathrm{O}}^\times}}-2\ln\frac{x_{\mathrm{Ce}_{\mathrm{Ce}}^\times}}{y_{\mathrm{Ce}_{\mathrm{Ce}}^\times}}+\frac{g_R}{k_BT}\,, \tag{A1}$$

$$\chi_b=\ln\left[\frac{x_{V_{\mathrm{O}}^{\cdot\cdot}}}{\mathcal{F}_{V_{\mathrm{O}}^{\cdot\cdot}}}\frac{x_{\mathrm{Ce}'_{\mathrm{Ce}}}}{\mathcal{F}_{\mathrm{Ce}'_{\mathrm{Ce}}}}\frac{\mathcal{F}_{V_{\mathrm{O}}^{\cdot}}}{x_{V_{\mathrm{O}}^{\cdot}}}\right]-\ln\frac{x_{\mathrm{Ce}_{\mathrm{Ce}}^\times}}{y_{\mathrm{Ce}_{\mathrm{Ce}}^\times}}+\frac{g_2}{k_BT}\,, \tag{A2}$$

$$\chi_c=\ln\left[\frac{x_{(\mathrm{Ce}V_{\mathrm{O}})^{\cdot}}}{\mathcal{F}_{(\mathrm{Ce}V_{\mathrm{O}})^{\cdot}}}\frac{\mathcal{F}_{V_{\mathrm{O}}^{\cdot\cdot}}}{x_{V_{\mathrm{O}}^{\cdot\cdot}}}\frac{\mathcal{F}_{\mathrm{Ce}'_{\mathrm{Ce}}}}{x_{\mathrm{Ce}'_{\mathrm{Ce}}}}\right]+\frac{g_{B1}}{k_BT}\,, \tag{A3}$$

$$\chi_d=\ln\left[\frac{x_{(\mathrm{Ce}V_{\mathrm{O}})^{\times}}}{\mathcal{F}_{(\mathrm{Ce}V_{\mathrm{O}})^{\times}}}\frac{\mathcal{F}_{V_{\mathrm{O}}^{\cdot}}}{x_{V_{\mathrm{O}}^{\cdot}}}\frac{\mathcal{F}_{\mathrm{Ce}'_{\mathrm{Ce}}}}{x_{\mathrm{Ce}'_{\mathrm{Ce}}}}\right]+\frac{g_{B2}}{k_BT}\,, \tag{A4}$$

$$\chi_e = 2x_{V_O^{\cdot\cdot}} + x_{V_O^{\cdot}} + x_{(CeV_O)^{\cdot}} - x_{Ce'_{Ce}} , \quad \text{(A5)}$$

$$\chi_f = x^{max}_{Ce^{\times}_{Ce}} - x_{Ce^{\times}_{Ce}} - x_{Ce'_{Ce}} - x_{(CeV_O)^{\cdot}} - x_{(CeV_O)^{\times}} , \quad \text{(A6)}$$

$$\chi_g = x^{max}_{O^{\times}_{O}} - x_{O^{\times}_{O}} - x_{V_O^{\cdot\cdot}} - x_{V_O^{\cdot}} - x_{(CeV_O)^{\cdot}} - x_{(CeV_O)^{\times}} \quad \text{(A7)}$$

and define

$$\chi^2_{total} = \sum_{\xi=a}^{g} A_\xi \chi^2_\xi , \quad \text{(A8)}$$

where A_ξ's are user defined weighting factors. It is clear that χ^2_{total} would be zero if the exact solution x_α values are substituted into Eqs. (A1)–(A8). On the other hand, χ^2_{total} would have a value larger than zero if any other x_a value is used. The closer these x_α values are to the actual solutions, the smaller χ^2_{total} is. Accordingly, the original problem of calculating the defect concentrations now becomes one of minimizing χ^2_{total} with respect to a set of x_α variables.

To accomplish this task, the algorithm adopted in this work first makes an initial estimate of the x_α values at the limit of low concentrations using the simpler traditional formulation described by Eqs. (64)–(67), and Eqs. (51)–(53). Utilizing the well-known procedures introduced by Brouwer[4,5,71] the approximate defect concentrations can be calculated at a conveniently chosen P_{O_2} (a value of 1 atm is typically used in this work). This set of x_α values is then used as the initial input to Eqs. (A1)–(A8). Using a conjugate gradient routine[30] the x_α values are then iteratively refined to minimize χ^2_{total}. In a typical run $\chi^2_{total} < 10^{-13}$ can be achieved within a few tens of iterations. The resulting x_α solutions are in turn used as the initial input to a new calculation at a slightly different P_{O_2}. In this manner, the defect concentrations may be calculated over a range of P_{O_2} at a fixed T. By trial and error it was found that the computation speed is optimized with $A_\xi = 1$ for $\xi = a$ to d, and $A_\xi = 1000$ for $\xi = e$ to g. This choice of the weighting factors apparently gives more weight to the effects of charge neutrality and structural conservation constraints (i.e., $\xi = e$ to g) and thus facilitates faster convergence.

[1] *Point Defects in Solids,* edited by J. H. Crawford, Jr. and L. M. Slifkin (Plenum, New York, 1972).

[2] *Crystal Lattice Defects and Amorphous Materials; Proceedings of the International Conference on Defects in Insulating Crystals,* edited by R. Smoluchowski (Gordon and Breach, New York, 1985).

[3] Special issue of MRS Bull. on Point Defects, vol. XVI, Nov. 1991.

[4] F. A. Kröger and H. J. Vink, in *Solid State Physics: Advances in Research and Applications,* edited by F. Seitz and D. Turnbull (Academic, New York, 1956), Vol. 3, p. 307.

[5] F. A. Kröger, *The Chemistry of Imperfect Crystals* (North-Holland, New York, 1964).

[6] A. D. Franklin, in *Point Defects in Solids,* (Ref. 1), p. 1.

[7] R. A. Swalin, *Thermodynamics of Solids,* 2nd ed. (Wiley, New York, 1972).

[8] R. H. Fowler and E. A. Guggenheim, *Statistical Thermodynamics* (Cambridge University, London, 1939).

[9] A. B. Lidiard, Phys. Rev. **94**, 29 (1954).

[10] A. B. Lidiard, in *Encyclopedia of Physics,* edited by S. Flugge (Springer, Berlin, 1957), Vol. XX, p. 246.

[11] L. W. Barr and A. B. Lidiard, in *Physical Chemistry,* edited by H. Eyring (Academic, New York, 1970), Vol. X, p. 151.

[12] A. B. Lidiard, in *Crystals with the Fluorite Structure,* edited by W. Hayes (Clarendon, Oxford, 1974), p. 101.

[13] C. Wagner, in *Progress in Solid State Chemistry,* edited by J. O. McCaldin and G. Somorjai (Oxford, New York, 1975), Vol. 10, p. 3.

[14] A. S. Nowick, in *Diffusion in Crystalline Solids,* edited by G. E. Murch and A. S. Nowick (Academic, New York, 1984), p. 143.

[15] N. Q. Minh, J. Am. Ceram. Soc. **76**, 563 (1993).

[16] *Science and Technology of Zirconia,* Advances in Ceramics Vol. 3, edited by A. H. Heuer and L. W. Hobbs (American Ceramic Society, Columbus, OH, 1981).

[17] *Science and Technology of Zirconia II,* Advances in Ceramics Vol. 12, edited by N. Claussen, M. Rühle, and A. H. Heuer (American Ceramic Society, Columbus, OH, 1984).

[18] *Science and Technology of Zirconia III,* Advances in Ceramics Vol. 24, edited by S. Sōmiya, N. Yamamoto, and H. Yanagida (American Ceramic Society, Westerville, OH, 1988).

[19] H. Rau, J. Phys. Chem. Solids, **28**, 903 (1967).

[20] G. G. Libowitz, in *Reactivity of Solids; Proceedings of the 7th International Symposium on Reactivity of Solids, Bristol, 1972,* edited by J. Anderson, M. Roberts, and F. Stone (Chapman and Hall, London, 1972), p. 107.

[21] G. G. Libowitz, J. Solid State Chem. **1**, 50 (1969).

[22] J. B. Lightstone and G. G. Libowitz, J. Phys. Chem. Solids **30**, 1025 (1969).

[23] J. S. Anderson, in *The Chemistry of Extended Defects in Non-Metallic Solids,* edited by L. R. Eyring and M. O'Keeffe (North-Holland, Amsterdam, 1970), p. 1.

[24] *Principles of the Theory of Solids,* 2nd ed., edited by J. M. Ziman (Cambridge, London, 1972).

[25] F. K. Fong, in *Physics of Electrolytes, Transport Processes in Solid Electrolytes and in Electrodes* Vol. 1, edited by J. Hladik (Academic, New York, 1972), p. 79.

[26] L. M. Atlas, J. Phys. Chem. Solids **29**, 91 (1968).

[27] L. M. Atlas, J. Phys. Chem. Solids **29**, 1349 (1968).

[28] L. M. Atlas, in *The Chemistry of Extended Defects in Non-Metallic Solids,* edited by L. R. Eyring and M. O'Keefe (North-Holland, Amsterdam, 1970), p. 425.

[29] L. Manes, in *Nonstoichiometric Oxides,* edited by O. T. Sørensen (Academic, New York, 1981), p. 99.

[30] W. H. Press, B. P. Flannery, S. A. Teukolsky, and W. T. Vetterling, *Numerical Recipes* (Cambridge University, New York, 1986), Chap. 10, p. 274.

[31] D. J. M. Bevan and J. Kordis, J. Inorg. Nucl. Chem. **26**, 1509 (1964).

[32] P. Kofstad, *Nonstoichiometry, Diffusion, and Electrical Con-*

ductivity in Binary Metal Oxides (Wiley, New York, 1972).
[33]O. T. Sørensen, in *Nonstoichiometric Oxides,* edited by O. T. Sørensen (Academic, New York, 1981), p. 1.
[34]H. L. Tuller and A. S. Nowick, J. Phys. Chem. Solids **18**, 859 (1977).
[35]H. L. Tuller and A. S. Nowick, J. Electrochem. Soc. **126**, 209 (1979).
[36]H. L. Tuller, in *Nonstoichiometric Oxides* (Ref. 33), p. 271.
[37]H. L. Tuller and A. S. Nowick, J. Electrochem. Soc. **122**, 255 (1975).
[38]A. S. Nowick, in *Crystal Lattice Defects and Amorphous Materials; Proceedings of the International Conference on Defects in Insulating Crystals, Utah, 1984,* edited by F. Luty (Gordon and Breach, New York, 1985), Vol. 12, p. 1.
[39]R. N. Blumenthal, P. W. Leo, and R. J. Panlener, J. Electrochem. Soc. **118**, 123 (1971).
[40]M. A. Panhans and R. N. Blumenthal, *Solid State Ionics,* **60**, 279 (1993).
[41]R. W. G. Wyckoff, *Crystal Structures,* Structures of the Compounds RX_2 Vol. I, 2nd ed. (Krieger, Malabar, FL, 1982) Chap. IV, p. 241.
[42]J-H Park and R. N. Blumenthal, J. Electrochem. Soc. **136**, 2867 (1989).
[43]S. Ling, M. P. Anderson, and T. A. Ramanarayanan, Solid State Ionics **59**, 33 (1993).
[44]E. S. Machlin, *An Introduction to Aspects of Thermodynamics and Kinetics Relevant to Materials Science* (Giro, New York, 1991).
[45]J. Hladik, in *Physics of Electrolytes, Transport Processes in Solid Electrolytes and in Electrodes* Vol. 1, edited by J. Hladik (Academic, New York, 1972), p. 35.
[46]C. Kittle, *Introduction to Solid State Physics,* 4th ed. (Wiley, New York, 1974).
[47]C. R. A. Catlow, M. Dixon, and W. C. Mackrodt, in *Computer Simulation of Solids,* edited by C. R. A. Catlow and W. C. Mackrodt (Springer-Verlag, New York, 1982), p. 130.
[48]*Theory of Defects in Solids,* edited by A. M. Stoneham (Oxford, London, 1975).
[49]This was observed by the author in the work of Refs. 55–57.
[50]J. D. Jackson, *Classical Electrodynamics,* 2nd ed. (Wiley, New York, 1975).
[51]C. R. A. Catlow, J. Corish, K. M. Dillers, P. W. M. Jacobs, and M. J. Norgett, J. Phys. C **12**, 451 (1979).
[52]W. C. Mackrodt and R. F. Stewart, J. Phys. C **12**, 5015 (1979).
[53]*Computer Simulation of Solids,* edited by C. R. A. Catlow and W. C. Mackrodt (Springer-Verlag, New York, 1982).
[54]C. R. A. Catlow, Solid State Ionics **8**, 89 (1983).
[55]S. Ling and A. S. Nowick, Phys. Rev. B **40**, 3266 (1989).
[56]S. Ling, A. S. Nowick, A. N. Cormack, and C. R. A. Catlow, Appl. Phys. A **49**, 69 (1989).
[57]A. N. Cormack, C. R. A. Catlow, and S. Ling, Phys. Rev. B **40**, 3278 (1989).
[58]R. Gerhardt-Anderson and A. S. Nowick, in *Transport in Nonstoichiometric Compounds,* edited by G. Simkovich and V. S. Stubican (Plenum, New York, 1985), p. 111.
[59]V. Butler, C. R. A. Catlow, B. E. F. Fender, and J. H. Harding, Solid State Ionics **8**, 109 (1983).
[60]R. W. Grimes and C. R. A. Catlow, J. Am. Ceram. Soc. **73**, 3251 (1990).
[61]M. Tosi, in *Solid State Physics: Advances in Research and Applications,* edited by F. Seitz and D. Turnbull (Academic, New York, 1964), Vol. 16, p. 1.
[62]L. Manes, C. M. Mari, and I. Ray, in *Thermodynamics of Nuclear Materials, Proceedings of the International Symposium 1979* (IAEA, Vienna, 1980) p. 405.
[63]E. A. Guggenheim, *Thermodynamics,* 5th ed. (North-Holland, Amsterdam, 1967).
[64]C. H. P. Lupis, *Chemical Thermodynamics of Materials* (North-Holland, New York, 1983).
[65]C. H. P. Lupis, *Chemical Thermodynamics of Materials* (Ref. 64), Chap. IV, p. 108.
[66]D. Y. Wang, D. S. Park, J. Griffith, and A. S. Nowick, Solid State Ionics **2**, 95 (1981).
[67]R. J. Panlener, R. N. Blumenthal, and J. E. Garnier, J. Phys. Chem. Solids **36**, 1213 (1975).
[68]B. Iwasaki and T. Katsura, Bull. Chem. Soc. Jpn. **44**, 1297 (1971).
[69]O. T. Sørensen, J. Solid State Chem. **18**, 217 (1976).
[70]R. J. Friauf, in *Physics of Electrolytes* (Ref. 45), p. 153.
[71]G. Brouwer, Philips Res. Rep. **9**, 366 (1954).
[72]M. Spears (private communication).